Hydrothermal Processing of Aqueous Biomass:
Process Development and Integration of a Novel Heating Technique.

A THESIS
SUBMITTED TO THE FACULTY OF THE GRADUATE SCHOOL
OF THE UNIVERSITY OF MINNESOTA
BY

Michael John Mohr

IN PARTIAL FULFILLMENT OF THE REQUIREMENTS
FOR THE DEGREE OF
MASTER OF SCIENCE

Roger Ruan

July 2013

Acknowledgements

I am grateful for the wealth of talent, skill and vision that the students, faculty and staff at the University of Minnesota exemplify. They embody the principles which all higher educational institutions strive for. Our shared accomplishments outlined within this work were truly a team effort. The vision for a renewably fueled future pursued and supported by our research partners at the Metropolitan Wastewater Treatment Plant and staff at UMORE Park was equally outstanding.

Although attempts to express my gratitude for the hard work and un-yielding support of this work cannot due them justice, I would like to acknowledge those with close ties to this project which directly influenced its outcome. First and foremost my advisor Professor Roger Ruan deserves a whole-hearted *Thank You*. Not only for the countless hours we discussed and refined this project, but for accepting and mentoring me in the first place. An associate professor in our lab, Dr. Paul Chen, also deserves recognition and thanks for not only his excellent administrative and advisory contributions, but also the often over-looked grant writing process.

My time as a graduate student within Dr. Ruan's lab has allowed me to explore and contribute to a vast number of renewable energy platforms, a luxury rarely experienced in today's educational systems. I would also like to thank Dr. Min Min, Dr. Shaobo Deng, Dr. Zhenyi (Jack) Du, Richard Griffith and Dave Hultman. I consider these individuals paramount to this project's success. Whether it was kind words of encouragement, afternoon brain-storming sessions, material suggestions, or reflections on experimental results, I'm confident I could not find a better support network associated with this great University.

My friends and family most certainly deserve credit here as well. The financial, emotional and intellectual support I received from them helped guide me through this process. I am grateful to have such outstanding family and friends standing in my corner. Again, my gratitude for their support cannot truly justify the importance of their influence.

Table of Contents

List of Tables

List of Equations

List of Figures

INTRODUCTION

This narrative aims to identify and address key bottlenecks in the scaling-up of an advanced multi-step algae-to-biofuel production system from conception to demonstration scale. Previous research carried out by Dr. Ruan's algae research group has identified robust algal strains capable of simultaneous wastewater treatment and highly productive biomass accumulation. Successful trials of these strains have been carried out in the laboratory (~1.0 L) and pilot-scale (~300.0 L) phases. Additionally, promising extraction and thermo-chemical conversion methods have been developed to fully utilize this promising renewable biomass resource. Research carried out within the University of Minnesota's Center for Biorefining, as well as, with colleagues at UMORE Park in Rosemount, MN will also be discussed.

Pilot-scale facilities at a wastewater treatment plant have shown the efficacy of cultivating algae on highly concentrated waste streams. Over the last four years our group has partnered with the Metropolitan Council to demonstrate the capability of cultivating algae solely within a concentrated wastewater media. The Metropolitan Wastewater Treatment Plant, located near Pig's Eye Lake in St. Paul, MN is one of the largest wastewater treatment facilities in the United States. Here, unmodified natural algal strains have demonstrated a capability to remove excess nutrients from a highly concentrated waste stream derived from dewatered sludge during the normal wastewater treatment process. Field trials using artificial and naturally light supplied to specially designed photobioreactors (PBR), a structure used to cultivate algae, have supplied an operational blueprint for demonstration-scale facilities now located at UMORE Park. Operational production knowledge gained from these pilot-scale studies has driven downstream processing technologies. Consequently, a robust thermochemical conversion process has been pursued to more readily process the resultant algal biomass.

Our research group has been developing advanced extraction, pyrolytic and hydrothermal conversion technologies specially tailored to compliment biomass produced from previous pilot-scale studies. Highly productive algal biomass is rapidly becoming one of the premier feedstocks utilized for renewable biofuel and biochemical production. Building on previous algal energy crop cultivation research, an advanced hydrothermal

conversion system was developed to process this promising resource. The ultimate goal of this current work is to develop a novel and robust hydrothermal liquefaction system to process algal and other compatible aqueous biomass resources into high value products. The advantages of hydrothermal processing, our over-all system development, and component optimization will be explored in later sections.

Ultimately, our group aims to produce a fully operational algae-to-biofuels test-bed platform. To reduce costs and improve the ecological and environmental performance of such a system, diluted anaerobically digested hog manure will be supplied as both a carbon on nutrient source for the cultivation system at demonstration. As the algal culture matures it simultaneously treats the agricultural wastewater, fixes carbon dioxide and provides an ideal energy and protein-rich resource for downstream food and fuel production systems. To achieve harmony between low-cost cultivation, wastewater treatment and downstream hydrothermal processing we have made many improvements to our overall algae-to-biofuels scheme.

LITERATURE REVIEW

1.1 Current Transportation Fuel Background.

1.1.1 Overview of U.S. Demand and Supply Trends.

Unprecedented demand in the twenty-first century for petroleum derived transportation fuels is driving up the cost of this essential resource. A reflection of this reality is acutely indicated by recent baseline price adjustments from the International Energy Agency. Their goal is to project petroleum market prices out to the year 2050. In the year 2000, the baseline price a barrel of oil was estimated at $33; by 2004 that figure rose to $40/barrel and by 2005 it ballooned to $55/barrel (Small & Dender, 2007). This startling trend reflects a rapidly growing demand of transportation fuels which are primarily sourced from petroleum crude. Data compiled from a 2012 *Annual Energy Overview Report* for the United States published by the Energy Information Administration outlines the steady increase in petroleum consumption over last few decades. As observed from figure 1, net petroleum imports have rising significantly to

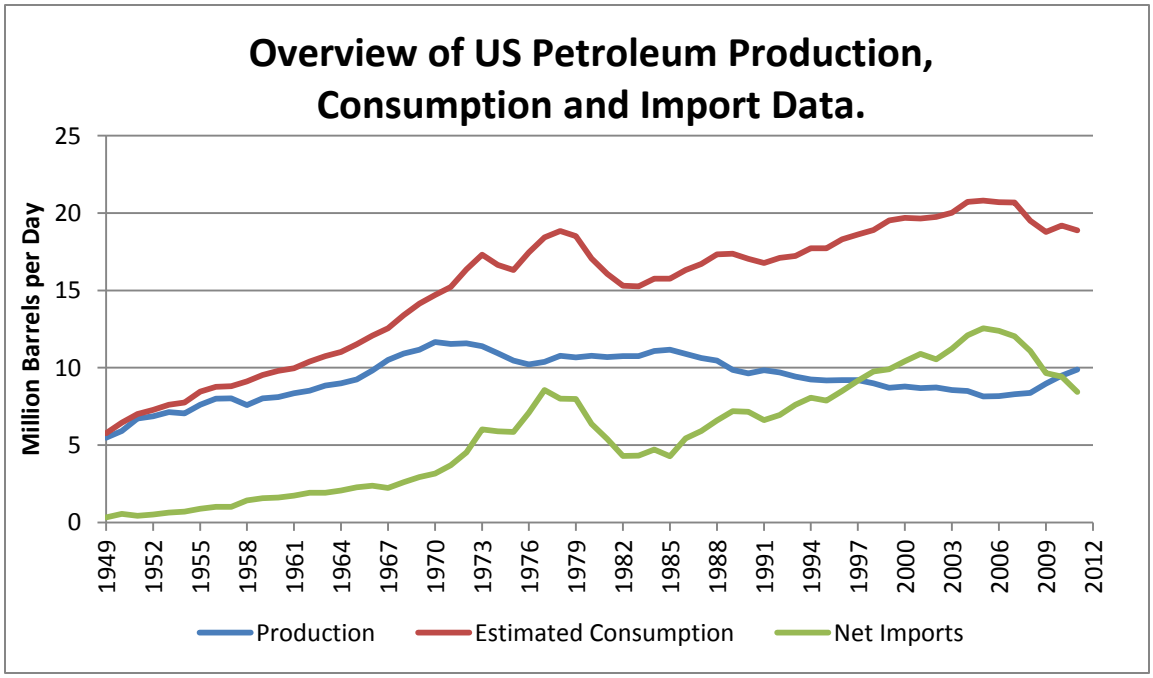

Figure 1. Historical overview of the net production, consumption and imports of petroleum products (U.S. Energy Information Administration, 2012).

offset recent declines in domestic production. Additionally, global consumption, especially in developing economies, has steadily increased further pressuring petroleum markets. To exacerbate this trend many energy experts believe that peak oil, the point at which maximum extraction takes places, will occur sometime within this century (Kharecha & Hansen, 2008). With once abundant supplies quickly dwindling and production numbers leveling off, transportation fuel prices are poised to continue their steep rise.

1.1.2 GHG Emissions from Transportation Fuels.

Concerns over greenhouse gas emissions (GHG) resulting from the combustion of petroleum resources are driving researchers and engineers to identify and develop green drop-in ready liquid fuel alternatives. Rising global temperatures driven primarily by an enhanced greenhouse effect from elevated greenhouse gas concentrations threatens to disrupt many of the Earth's sensitive ecosystems. Using numbers published by Brandt & Farrell, one can derive the estimated total carbon emissions from one barrel of oil which when released contribute to the enhanced greenhouse effect. Data from the year 2005 reveals that roughly 3.2 GtC of carbon were emitted from 29.3 Gbbl (29.3 billion) barrels

of petroleum crude consumed that year globally (Brandt & Farrell, 2007). Using an atmospheric carbon dioxide equivalent of 1.0 ppm atmospheric [CO2]: ~2.12 GtC; the carbon emissions released solely from petroleum in 2005 resulted in a 1.51 ppm increase in atmospheric CO2 concentrations (Kharecha & Hansen, 2008). Clearly, carbon emissions derived directly from petroleum fuels will continue to considerably contribute to global climate change if no action is taken. Armed with this knowledge researchers and policy makers around the world have begun an ambitious effort to significantly reduce or eliminate GHG emissions from transportation fuels altogether.

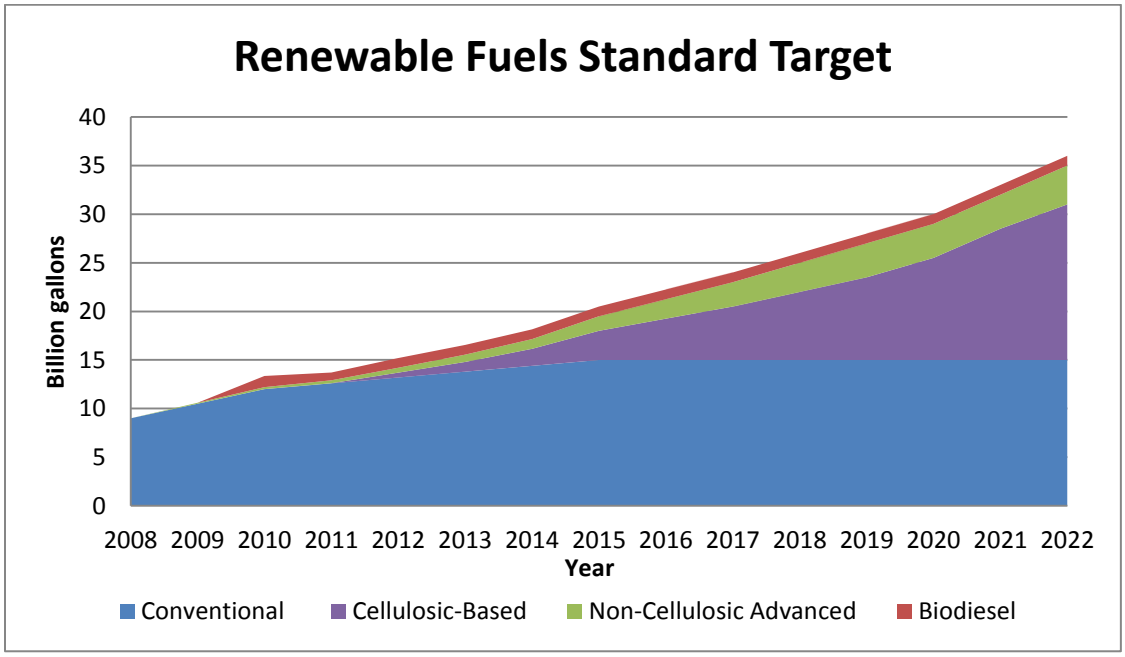

Figure 2. Renewable Fuels standard targets (Schnepf & Yacobucci, 2010).

1.2 EISA of 2007 and Research Motivations.

In 2007 the United States congress laid out an ambitious framework to help wean the nation from petroleum-derived fossil fuels to greener renewable biofuel platforms. Significant investments in advanced and cellulosic biofuel projects involving enzymatic lignocellulosic pretreatment, algal lipid production, pyrolytic conversion, advanced microbial engineering and slew of others have been funded in recent years. The Energy Independence and Security Act (EISA) of 2007 laid the foundation for the production of nearly 36 billion gallons of renewably-derived biofuels by the year 2022. In addition to reducing our nation's dependence on dwindling petroleum reserves, the EISA also

mandates significant GHG emission reductions of 20%, 50% and 60% for biofuels classified as renewable, advanced and cellulosic respectively. Figure 2 outlines the biofuel targets set forth by the Environmental Protection Agency's Renewable Fuel Standards (RFS) in response to the 2007 EISA mandate. A production cap of 15 billion gallons per year of conventional cornstarch-based ethanol is set to restrict market perturbations as corn is increasingly used as a fuel rather and food resource. This restriction is also meant to purposefully stimulate growth and innovation in the much more difficult to develop advanced and cellulosic biofuel divisions.

1.2.1 Biofuel Categories

Conventional corn starch-based ethanol production has already met its production quota of 15 billion gallons per year while other advanced *cellulosic* and *non-cellulosic* varieties encouraged by the RFS have significantly lagged. Advanced biofuels are defined as any renewable fuel which achieves at least a fifty percent reduction in life-time greenhouse gas emissions compared to its petroleum counterpart. Cellulosic biofuels are those derived from lignocellulosic plant materials such as grasses, woody residue, leaves, ect. The production of these biofuels has been substantially hindered by the lignocellulosic barrier resulting in high pre-treatment costs which substantially limit their industrial scale production. Increased biodiesel production is limited, in part by the requirement of high-value food stocks such as soybean or sunflower oils. The non-cellulosic biofuel category is set to accommodate any future advanced fuel which might not fit into another category. Depending on how algal biomass is converted, the subsequent biofuel could fall into any of the non-conventional biofuel categories outlined above. Section 1.3.0 will outline algal derive biofuels in greater detail.

1.2.2 Anticipated EISA Impacts.

The EPA has outlined a few anticipated outcomes of the EISA initiative. By the year 2022, the 36 billion gallons of biofuels produced annually is suspected to displace around seven percent of the liquid transportation fuels required in the U.S. The impacts of conventional cornstarch-based biofuels are estimated to decrease total corn exports less than eight percent; the resultant supply strain is excepted to minimally bump up food

prices by ~$10 annually (Office of Transportation and Air Quality., 2010). A significant reduction in greenhouse gas emissions will also accompany the economic benefits of increased biofuel production.

1.3 Algae as a Feedstock for Advanced Biofuel Production.

1.3.1 Advantages of Algal Feedstock.

Since the late 1950's researchers have pondered algae's ability to provide a low cost feedstock for renewable biofuel production. It was not until the early 1970's that serious research took place on algae's ability to meet rising energy needs. In 1978 the US Department of Energy initialized the Aquatic Species Program (ASP), in part to study algae's potential to meet increasing gas shortages (Chen, et al., 2009). Before shutting down in the late 1990's the ASP produced a report in 1998 outlining key challenges that must be overcome for algal-based fuels to reach pump parity with their petroleum counterparts. The release of that report signified an end to the 18 year program, at which time gas and oil prices were at historic lows. Interestingly, today a renaissance in algae cultivation and conversion has once again taken place. A recent *Greentech Innovations* report lists over 53 major players in the algal industry in 2009 (GTM Research, 2009). Since that time interest in algae has continued to rise.

Algae offer many advantages for liquid biofuel production over their terrestrial land counterparts. They can be characterized as "remarkable and efficient biological factories capable of taking a waste form of carbon (CO_2) and converting it into high energy density compounds" (Sheehan, Dunahay, Benemann, & Paul, 1998). A bullet list of the universally cited advantages is provided below (U.S. DOE., 2010).

- Algae are potentially much more productive on per acre basis than terrestrial land plants.
- Large-scale cultivation can be carried out on non-arable land with waste nutrients, thus relieving pressure on traditional land crops.
- Algae can be cultivated on non-potable water. They can grow within wastewater, brackish or saline media.
- As algae grow they fix CO_2 into energy dense products. This offers an attractive incentive to co-locate with large industrial emitters.
- Raw algal biomass offers a large biorefining potential. A wide variety of fuels and high-value co-products can be produced.
- Robust, rapidly maturing cell culture can tolerate environmental stresses.

Algae are often promoted as an ideal next generation biofuel feedstock because they can produce intracellular lipid droplets which are high-density energy storage molecules that can be readily converted into biodiesel. Promising algal strains can readily obtain over 40 percent of their mass in lipid form, thus providing 5,000-10,000 gallons of algal oil per acre per year. By comparison, optimal soybean oil yields peak around 50 gallons per acre per year, while palm can produce about 650 gallons per acre per year (GTM Research, 2009). Additionally, algae cells contain large amounts of starch, protein and other metabolites such as carotenoids, omega-3 fatty acids, etc. (Chen, et al., 2009). These important compounds can be utilized as high-value nutraceuticals, animal feed or for producing additional non-fuel products. Clearly, algal cultivation will play an important role in helping future generations meet increasing food, chemical and energy supply challenges. Fortuitously, large-scale algae production systems can complement rather than compete with existing agricultural crops and practices by using land and water resources that today are under-utilized.

1.3.2 Algae-based Biofuels.

Algal biomass can be converted into biofuels in a few ways. The most common form of biofuel derived from algae is biodiesel. Energy-dense triglycerides, the main components of high-lipid algae, are extracted and converted in a process called trans-esterification into biodiesel. Unfortunately, extracting the oil in algae is expensive and difficult to carry out. Furthermore, the trans-esterification process is sensitive to high concentrations of free fatty acids and excess water, both of which are abundant in oil derived from algal biomass. Along more traditional lines, cellulose and starch from the algal biomass can also be fermented biochemically into alcohols; in this case cellulosic algal-derived biofuels can be produced in much the same way conventional ethanol is fermented from corn-starch. Thermochemical conversion technologies have also been explored to process wet and dry algal biomass into energy-dense bio-oils. All liquid fuels derived from algal biomass, regardless of conversion technique or technology, are considered advanced *non-conventional* biofuels; however, tax credits and other production incentives have yet to be awarded to algal-based fuels.

To increase the production incentives of algal-based fuels the Renewable Fuel Parity Act of 2011 has been introduced to include all algal fuel into the same proposed 'feedstock neutral' category of advanced biofuel under revised language for subsequent RFS publications (112th Congress 1st Session, 2011). Section 1.4 will briefly highlight the production and properties of these fuels.

1.4 Biochemical Processing of Algae into Biodiesel and Ethanol.

1.4.1 Biodiesel from Microalgae.

Algae are capable of producing a large amount of energy-dense lipid bodies within their cells. These lipids are more commonly known as triacylglycerols or TAGs and can be readily converted to biodiesel. Like the traditional oilseed crops of soybean, rapeseed and palm, algae produce TAGs with the characteristic glycerol backbone supporting three long-chain fatty acids. Unmodified TAGs can be used directly as an alternative fuel; however, they are limited to stationary applications due to their high viscosity and inferior combustion characteristics when utilized in modern diesel engines. Consequently, a simple chemical modification is employed to cleave TAGs into three alkyl esters using simple alcohols in the presence of a catalyst (Sheehan, Dunahay, Benemann, & Paul, 1998). The process, widely referred to as *transesterification*, is now commonly practiced to convert oil-crop TAG's into high quality biodiesel; however, transforming algal TAGs into biodiesel does have its limitations.

Sharma & Singh (2009) outline important variables affecting the quality of the resultant biodiesel from algal TAGs. Most important is the original oil composition and its free fatty acid content (FFA). FFA are described as "saturated or unsaturated monocarboxylic acids that occur naturally in fats, oils or grease, but are not attached to glycerol backbones" (Sharma & Singh, 2009). Large amounts of FFA lead to increased acid values in the final biodiesel product and can cause saponification if free water molecules are present. When initial FFA content is sufficiently low (<1%), a one-step alkaline-catalyzed transesterification process can be used, however, if FFA content is high, a more expensive and slower acid-catalyzed two-step process must be used (Sharma & Singh, 2009). High water content, regardless of the presence of alkaline or acid catalysts, interferes with the conversion of TAGs to biodiesel. For this reason, large-scale

algal-derived biodiesel production plants are presently limited. More research is needed in reducing the FFA content of native algae or pursing in-situ transesterification technologies that overcome algae's significant water content barriers before economically acceptable processes covert their TAG portions to useable fuels.

1.4.2 Fermentation of Algal Biomass into Alcohol.

Starch and cellulose constitute a large, if not majority, amount of intracellular mass within a given algae cell. These simple carbohydrates are ideal candidates for sugar fermentation. To utilize the carbohydrate portion of algae, the feedstock must first be dried and ground into a powder to destroy the cell wall. Mechanical and enzymatic extraction processes have been developed to increase sugar accessibility (Amin, 2009). After extraction and hydrolysis create monomeric sugars, yeasts can be used to ferment the carbohydrates into simple alcohols like ethanol. Recent studies reveal that up to 27% of intracellular microalgae starch within the microalgae can be fermented by yeast within 24 hours. Typical fermentation products of carbon dioxide, acetate, ethanol and hydrogen where detected (Ueno, Kurano, & Miyachi, 1998). After fermentation, the alcohol containing slurry must be pumped to a distillation unit where water and the alcohol are separated. Like conventional ethanol production processes, this separation step consumes much of the process energy required to produce the biofuel which significantly detracts from the overall net energy gain derived from the process.

Biochemical processing of algal biomass has been explored in previous studies. Researches have been able to successfully convert high-lipid algal biomass into good quality biodiesel. Algal-derived biodiesel displays many of the same properties as its petroleum counterpart. Similar heating values (~41 MJ kg^{-1}), H/C ratios (1.81), density (0.864 kg l^{-1}), and viscosity (5.2 cSt at 40 °C) can be obtained (Xu, Miao, & Wu, 2006). Unfortunately, the high cost of specialized catalysts capable of accommodating high water content and the relatively large FFA content of most microalgae feedstocks severely limits this conversion technique. Exacerbating this reality, low cost and efficient lipid extraction technologies are hard to come by. Most often algae are expeller pressed and lipids are extracted with organic solvents such as chloroform, hexane, or methanol. This method is costly and fairly non-specific, often times non-lipid components are

extracted which complicates downstream processing. Large-scale fermentation of algal biomass is plagued by similar issues. The relatively low alcohol productivity coupled with high distillation costs has discouraged large-scale fermentation studies of microalgae biomass to lab trials. In the next section, more suitable thermochemical processing technologies will be introduced to convert algal biomass into high value products.

1.5 Thermochemical Processing of Algae.

1.5.1 Introduction to Thermochemical Processing.

Thermochemical processing of biomass generally converts the whole algal cell or residues from prior extraction methods into energy dense products. The three most typical processing techniques are gasification, pyrolysis and hydrothermal liquefaction. Typical thermochemical products include: syngas, bio-oil, biopolyols and bio-char. Syngas is typically burned in combustion applications to produce heat and electricity. Bio-oil finds uses in stationary burner applications or can be upgraded into transportation fuels. Biopolyols can be used for downstream material synthesis. Finally, bio-char is readily used as a soil enricher and is widely held as an excellent carbon sequestration mechanism (Chen, et al., 2009). Thermochemical processing is typically characterized by fast and efficient conversions of organic biomass into energy-dense products; however, limited work has been carried out utilizing microalgal feedstocks because of limited biomass supply.

1.5.2 Gasification.

Processing biomass in extreme temperatures (800-1000°C) under partially oxidizing conditions will yield a combustible gas known as syngas. The composition of syngas can vary widely depending on the properties of the parent feedstock as well as with the type of gasifier utilized; however, it is generally comprised of simple reduced compounds of H_2, CH_4, CO, and NH_3. Syngas (heating value ~4-6 MJ/N m^3) is typically burned to provide heat and electricity and has been promoted in highly efficient gas turbines combined with steam generators to increase its energy utility. High quality cleaned syngas can also be used as feedstock for the production of methanol and other important chemical building blocks (McKendry, 2002). Limited studies converting

microalgae feedstock into syngas have been carried out. Anticipated observations of H_2, CH_4, CO, and CO_2 were measured when microalgae *Chlorella protothecoides* was gasified in 551- 951 °C temperatures. Using this feedstock it was demonstrated that a syngas composing of 57.6% H_2 by volume is achievable (Demirbas A. , 2010). Nevertheless the efficacy of utilizing gasification as a thermochemical conversion method of microalgae is limited. The biomass must be dried before conversion which imposes a large energetic penalty to the process.

1.5.3 Pyrolysis.

Pyrolysis is the thermochemical decomposition of dry organic biomass in the complete absence of oxygen into bio-oil, bio-char and syngas at temperatures between 300-600 °C. Biomass is typically heated though direct contact in fluidized sand or other heated surfaces. Like gasification, pyrolysis products are greatly influenced by parent feedstock composition, reactor design, process temperature and reaction time. Resultant syngas can be directly combusted or upgraded, chars find utility as soil amendments and bio-oil is highly sought after for its significant transport fuel potential. A summary of various pyrolytic conditions and the typical resultant products are outlined in Table 1.

Method	**Residence Time**	**Temp (K)**	**Heating Rate**	**Products**
Carbonation (Slow)	Days	675	Very Low	Charcoal
Conventional	5-30 min	875	Low	Oil, Gas, Char
Fast	0.5-5.0 s	925	Very High	Bio-oil
Flash-liquid (From flash pyrolysis)	<1.0 s	<925	High	Bio-oil
Flash-gas (From flash pyrolysis)	<1.0 s	<925	High	Chemical, Gas
Hydro-pyrolysis (with water)	<10.0 s	<775	High	Bio-oil
Methano-pyrolysis (with Methanol)	<10.0 s	>975	High	Chemicals
Ultra	<0.5 s	1275	Very High	Chemicals, gas
Vacuum	2-30 s	675	Medium	Bio-oil

Table 1. Summary of various pyrolysis parameters and product yields (Demirbas A., 2009).

Over the last few years two general categories of pyrolysis have become commonly recognized. The first, conventional pyrolysis operates at lower temperatures and longer residence times and results in primarily bio-char production. The second, fast pyrolysis, utilizes very high heating rates coupled with short residence times and rapid cooling to achieve primarily condensable gas (bio-oil) products. Given the higher throughput, increased product yields and enhanced upgrading potential of bio-oils; fast pyrolysis has been increasingly promoted as a next generation renewable energy platform (Chen, et al., 2009). Bio-oil produced by fast pyrolysis has a heating value of around 16 MJ/kg compared to diesel's 43 MJ/kg (Demirbas, Balat, & Balat, 2011). This relatively high heating value gives bio-oil a very promising future as a primary fuel for heat and power generation facilities.

The pyrolysis of algae converts the entire cellular matrix into energy dense products. Lipid, protein and carbohydrate components are readily converted into bio-oil, while combustible char and syngas products can also be produced (Ginzburg, 1993). Pyrolysis of algae produced a bio-oil of higher quality (with heating values around 29 MJ/kg and lower oxygen content) and quantity than from lignocellulosic feedstocks (Miao, Wu, & Yang, 2004). These results reflect the fact that algae lack complex and recalcitrant lignin structures which significantly reduce bio-oil production and overall quality. Additionally, algae's high initial lipid content promotes high quality bio-oils with comparable C/H ratios to those of heavy petroleum crude. The large-scale adoption of pyrolysis to convert algae to bio-oil has been hindered by the necessity of first drying the biomass. Like gasification this step introduces large energetic loses to the conversion scheme. Bio-oils derived from microalgae, although simpler than those from lignocellulosic biomass, still contain complex and unstable compounds which inhibit their long-term storage and upgrading potential.

1.5.4 Hydrothermal Processing.

Hydrothermal processing (HP) was born out of the need to convert aqueous biomass resources without necessitating the costly energetic step of drying. On the most fundamental level, HP's goal is to replicate and enhance the extreme environmental conditions which transformed ancient biomass into petroleum crude. HP is carried out

under elevated temperatures between 200-700 °C with suitable pressures to keep the aqueous slurry in a single liquid state. Eliminating the liquid-to-gas phase change results in considerable energetic savings that cannot otherwise be achieved using other thermochemical conversion platforms which require dry biomass. Additionally, the special properties of water under HP conditions can significantly enhance biomass reformation into energy dense products. Given the above information, HP technologies are uniquely well-suited for accommodating microalgae biomass. The following sections will outline the advantages of HP technologies, feedstock properties and important processing variables.

1.5.5 HP Conditions.

Hydrothermal processing can be carried out under an array of conditions. In general, three distinct HP regions can be delineated based on the conversion media's temperature and pressure. The three regions, highlighted in figure 3, are based on water's sub or supercritical phase characteristics and are detailed below:

1. Liquefaction- Moderate temperature 150-374 °C with suitable pressures 2-30 MPa. Pressure is greater than water vapor pressure to inhibit liquid-to-gas phase change. Water is in a sub-critical state under these conditions. This region produces primarily bio-oil products.
2. Catalytic Gasification- High temperature 374-550 °C under high pressure 22-35 MPa conditions. Water is in a supercritical condition in which partial gasification and thermolysis of biomass exists.
3. High-temperature Gasification- Extremely high temperature 550-700 °C under 22-35 MPa conditions. Complete biomass thermolysis and non-catalytic reformation occurs.

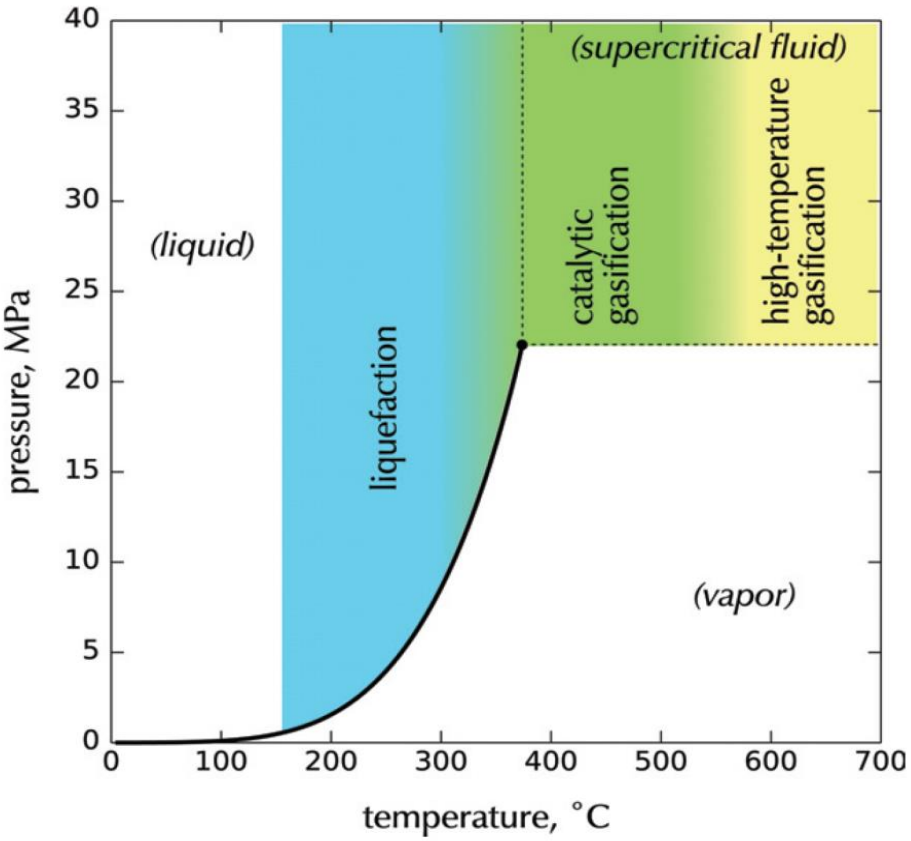

Figure 3. Hydrothermal processing phase diagram of water. Point (374 °C @ 22 MPa) highlights the supercritical point of water (Peterson, Vogel, R., Froling, Antal, & Tester, 2008).

1.6 Hydrothermal Liquefaction: A Review.

1.6.1 Introduction to Hydrothermal Liquefaction.

Hydrothermal liquefaction (HTL) is a promising subset of the traditional HP thermochemical conversion process. HTL is carried out primarily within an aqueous media under specific conditions which give water favorable solvation and heat transfer properties that aide in biomass reformation. Similar to pyrolysis, HTL processing can convert organic material into energy dense hydrocarbon materials. Products such as syngas, char, bio-oil and aqueous phase organics are typically produced; however, the yield and quality of the bio-oil under HTL conditions is often greater than those produced under pyrolytic conditions. Additionally, HTL accommodates wet biomass feedstocks, thus eliminating the energetically unfavorable step of drying encountered with pyrolysis.

The main scope of the following review will be focused on bio-oil production from HTL processing.

1.6.2 Characteristic of Subcritical Media.

Water's unique properties under subcritical conditions offer many important solvation and reaction benefits for biomass reformation. Figure 4 outlines the density, dielectric and self-ionization constants of water at 30 MPa over its sub and supercritical regions. These important properties change considerably as reaction temperatures increase from sub (0-374 °C) to supercritical (374-500 °C) conditions. The overall effects of these properties are outlined below:

- Density: The reduced density of water under subcritical conditions promotes fast and uniform reactions ideal for accommodating biomass particles. The compressibility of water under subcritical conditions, however, is still low compared to supercritical conditions, thus reducing processing costs.
- Dielectric Constant: Decreases rapidly from polar to non-polar region. This transformation occurs as water transitions from a highly hydrogen-bonded solvent at room temperature to one that represents a non-polar solvent at elevated temperatures (Peterson, Vogel, R., Froling, Antal, & Tester, 2008). This results in increased solubility of non-polar hydrophobic organic compounds which is especially advantageous when processing high-lipid containing feedstocks such as microalgae. The ionic solubility of salts also decreases under these conditions, offering an opportunity to selectively precipitate unwanted salts from the product streams.
- Self-ionization constant (K_w): The self-ionization constant, characterized as K_w ($K_w = [H_3O^+][OH^-]$), is an estimate of the number of available hydronium and hydroxide ions present within the media. A higher K_w promotes many acid and base-catalyzed reactions such as biomass hydrolysis (Toor, Rosendahl, & Rudolf, 2011).

Subcritical water also displays enhanced miscibility with gaseous compounds. This allows the HTL process to utilize reactive and inert gases to catalyze and stabilize

product yields. Additionally, homogenous and heterogeneous catalysts can be employed either directly in the solvent, or within the reaction vessel.

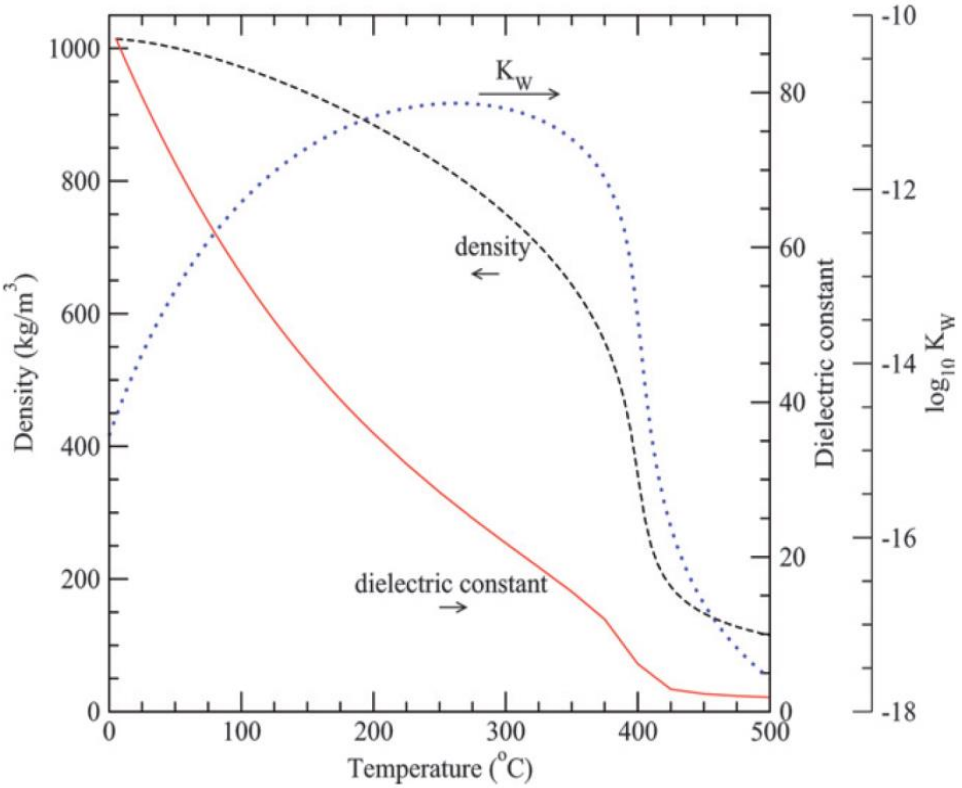

Figure 4. Density, dielectric and self-ionization constants of water at 30 MPa as a function of temperature (Peterson, Vogel, R., Froling, Antal, & Tester, 2008).

1.6.3 Advantages of HTL Conversion.

The primary advantage of the HTL over other thermochemical processing technologies is the accommodation of water. By converting biomass under subcritical conditions the considerable enthalpedic losses of vaporization and/or distillation can be avoided. Because hydrothermal liquefaction converts nearly all forms of aqueous organic material, a wide variety of biomasses as well as municipal and agricultural wastes can be utilized. The robust conversion process can transform nearly all organic feedstocks into energy-dense gas and liquid products. As outlined above, the unique properties of subcritical water also enhance biomass reformation and product separation. Finally, HTL has an enormous potential to transform costly bio-hazardous organics into useable

products. The high-temperature heat treatment of biomass ensures a >22D (0.1^22 survivors) destruction of infectious materials (Peterson, Vogel, R., Froling, Antal, & Tester, 2008).

1.6.4 Concerns of HTL Conversion.

The relatively high corrosivity of the reaction media under slightly polar and dense conditions results in significant acid pitting and stress corrosion to the reactor vessel materials. To overcome this issue expensive Nickel or Titanium based alloys must be used to ensure longevity and safety of the HTL device. Additionally, the decreased ionic solubility of HTL media can promote the precipitation of salts which can coat and clog sensitive reactor components. Energy recovery and heat recycling is difficult to achieve under HTL processing. Advanced heating and heat recovery methods could help to substantially reduce input processing costs.

1.7 Primary HTL Products.

1.7.1 Bio-crude.

Like pyrolysis, HTL's most sought after product is bio-oil also commonly referred to as bio-crude. The idea of converting organic feedstocks such as grasses, corn stover, microalgae and sawdust into bio-oil was first reported in 1944 by E. Berl. He was able to achieve a *petroleum-like* product when converting a variety of biomass resources under a subcritical (~230 °C) alkaline media. It was reported that the resultant bio-oil product contained 60% of the starting materials carbon while retaining 75% of its original energy content (Berl, 1944).

Research into the viability and conversion of organic matter into bio-oil has come and gone over the years since Berl's pioneering work. Typical hydrothermal liquefaction experiments are carried out in liquid water under 280-380 °C and 7-30 MPa conditions. In general, bulky energy-rich organic feedstocks with energy density of ~10-20 MJ kg^{-1} are converted into energy-dense bio-oils whose heating values range from 30-36 MJ kg^{-1}. Additionally, initial feedstock oxygen contents of 30-50% are reduced to 10-20% in the final bio-oil product (Peterson, Vogel, R., Froling, Antal, & Tester, 2008). This transformation represents that significant upgrading has been accomplished; however,

bio-oil's oxygen content and heating values are still inferior to those of petroleum crude (<1.0% O_2 and ~43 MJ kg^{-1}) (Aitani, 2004). The relatively high oxygen content in bio-oil renders it a poor candidate for downstream refining. One of the primary ongoing research goals within the HTL processing scene is to substantially decrease oxygen content without reducing its yield. Currently, HTL-derived bio-oil's tendency for polymerization coupled with its high corrosivity limit its applicability to exclusively stationary combustion sources (Peterson, Vogel, R., Froling, Antal, & Tester, 2008).

	Hydrothermal liquefaction	Fast pyrolysis
Moisture (wt%)	5	25
Elemental analysis (dry basis, wt%)		
C	77	58
H	8	6
O	12	36
Heating content (MJ kg^{-1})	35.7	22.6
Viscosity (cps)	15 000 @ 61 °C	59 @ 40 °C

Table 2. Elemental and physical comparison of HTL and fast-pyrolysis derived bio-oils. HHV values reported (Elliott & Schiefelbein, 1989).

Bio-oils derived from HTL offer many advantages over those from pyrolytic conversion platforms. HTL bio-oils generally have lower oxygen and moisture contents when compared to pyrolysis-derived bio-oils. This results in higher comparative heating values and lower corrosivity for HTL bio-oils. Additionally, HTL bio-oils contain fewer polar organic compounds which give them better long-term stability than pyrolytic bio-oils while also reducing their affinity for water (Peterson, Vogel, R., Froling, Antal, & Tester, 2008). In a distinction from pyrolysis, HTL processing also forms an aqueous organic-rich phase in which some of the initial feedstock oxygen and heating content ends up. Table 2 outlines key differences in bio-oils derived from similar feedstocks, but processed differently. In summary, HTL processing generally yields more bio-oil of a higher quality than from its pyrolytic companions.

1.7.2 Aqueous, Char and Gas Phases.

As stated earlier, a non-trivial amount of the initial heating value and oxygen content end up in the aqueous organic phase during HTL. This phase can often contain more than 18% and 20% of the respective initial feedstock heating and oxygen content (Goudriaan, et al., 2000). Additionally, a significant portion of the initial Nitrogen content ends up in the aqueous phase as polypeptide bonds are broken and protein components are solubilized. The char phase is quite similar to that produced during pyrolytic conversion, much of the initial inorganic and mineral content end up here. Reducing the char phase is another on-going effort within HTL research. By stabilizing intermediate degradation products with catalysts or process gases char formation can be significantly reduced. Under HTL conditions mainly CO_2 is produced in the gaseous phase. Carbon dioxide production is highly desired because oxygen is removed from the process this way, thus increasing the heating value of the bio-oil. Additionally, the removal of oxygen in the form of CO_2 over H_2O yields in a bio-oil product with a higher H:C ratio which increases the desired properties of the bio-oil product. Under super-critical conditions reduced gases such as H_2, CH_4 and CO are the predominate products after conversion.

1.8 Review of Important HTL Parameters for Optimal Bio-oil Production.

1.8.1 Temperature.

Temperature plays one of the most important roles during HTL processing. Not only does the final temperature define the solvation properties of the hydrothermal media, it also plays a direct role in the mechanics of biomass degradation. In its most elementary role, elevated temperatures above the required activation energies of bond disassociation aide in biomass depolymerization. This not only increases the concentration of free radicals, but also the probability of repolymerization of the fragmented species. The recombination of small molecular reactive species after depolymerization is what primarily leads to bio-oil formation. Toor et al. (2011) summarizes this phenomenon as the HTL *Universal Reaction Mechanism* which is outlined below:

1. High-temperatures result in depolymerization of biomass constituents into monomer units.
2. Decomposition of biomass monomers by cleavage into reactive units.
3. Recombination of reactive monomer products into bio-oil. Further heat treatment can lead to additional secondary fragmentations resulting in char formation.

The final reaction temperature imparts a significant impact on the distribution and quality of HTL products. Low temperatures (< 280 °C) inhibit biomass depolymerization resulting in poor bio-oil yields (Akhtar & Amin, 2011). Most often, low temperature thermochemical conversion coupled with longer residence times leads to significant char formation. This process is widely known as hydrothermal carbonization and can be useful for producing charcoal with reduced oxygen and nitrogen content. Conversely, high temperature environments (> 350 °C) promote increased gas and aqueous phase products. At these elevated temperatures secondary decomposition reactions take place which significantly reduce the production of bio-oil. In an analysis of various biomass feedstocks including microalgae, macroalgae, cattle manure, grassland perennials and eucalyptus optimal bio-oil yields were observed in the range of 300-360 °C (Akhtar & Amin, 2011). Each study revealed an ideal conversion temperature for each feedstock over the elevated temperature profiles studied.

Unsurprisingly, previous studies have shown a strong correlation between initial feedstock composition and the optimal temperature for bio-oil production. Compact biomass feedstocks such as microalgae are better reformed under higher temperature (~350 °C) conditions (Biller & Ross, 2011). Bulky lignocellulosic materials appear to more readily convert under less extreme conditions of ~300 °C (Zhang, Keitz, & Valentas, 2009). Biochemical variations in the chemical compositions of biomass feedstocks necessitates that researchers identify the optimal bio-oil forming temperature for each feedstock independently. HTL processes which convert mixed feedstocks that contain a multitude of diverse organic compounds must find a compromise between the ideal bio-oil forming temperatures for each component. In general, the optimum bio-oil forming temperatures appear to the range from 300-360 °C across most biomass resources.

1.8.2 Heating Rate.

Heating rates are suspected to play a similar role in HTL conversion as they do in other thermochemical conversion platforms. As observed from table 1, fast and flash pyrolysis employ extremely fast heating rates to achieve relatively high bio-oil yields. In general, higher heating rates support increased bulk fragmentation of biomass constituents while inhibiting char formation. This effect is semi-muted during HTL because fragmented species are better stabilized and dissolved in the subcritical media compared to the non-aqueous media during pyrolysis. Nonetheless bio-oil yields have shown significant improvement from 63% to 76% when heating rates from 5-140 °C min^{-1} where investigated using perennial grasses (Zhang, Keitz, & Valentas, 2009). In fact, the relationship was so profound that empirical regression analysis was performed to elucidate the optimal heating rate for this feedstock. The model created is listed below:

$$liquid\ yield(\%) = [0.0042 * \ln(heating\ rate) + 0.5514] * 100$$

Equation 1. Liquid Bio-oil yield based on heating rate (Zhang, Keitz, & Valentas, 2009).

As heating rates exceed those actively studied (140 °C min^{-1}), the model returns minimal benefits of increasing rates. In general higher heating rates improve bio-oil yields, the effects of extremely high heating rates in excess of 300 °C min^{-1} are absent in all HTL literature because the necessary equipment to reach those extreme rates does not exist. This has severely limited studies which hope to optimize heating rates during the HTL process.

Traditional HTL reactors exhibit relatively slow heating rates (5-10 °C min^{-1}) because they are carried out within thick walled stainless steel autoclaves during batch processes. Thus, heating rates are thermodynamically limited to the heat transfer properties of the heating source, vessel wall conduction and finally the heat conduction of processed media. Equation 2 outlines the combined conductive and convective heat transfer for a cylindrical vessel which approximates the characteristics of a standard HTL batch reactor (Singh & Heldman, 2008).

$$q = \frac{T_i - T_\infty}{\frac{1}{h_i A_i} + \frac{ln(r_o/r_i)}{2\pi Lk} + \frac{1}{h_o A_o}}$$

Equation 2: Combined Conductive and Convective Heat Transfer Equation (Singh & Heldman, 2008).

Enhancing the heating rate during conversion is severely limited by the convective (h_i and h_o) and conductive (k) coefficients of the heating source, process media and HTL reactor. Although the heating element and the subcritical media exhibit excellent heat transfer capabilities, the thickness of stainless steel autoclave walls and their resultant poor heat transfer coefficient limits the overall heat transfer efficiency. Even as researchers have increased the outer heating element's temperature, practical heat transfer limitations of the physical reactor vessel inhibit heating rates to < 100 °C min^{-1} thus eliminating the potential benefits of flash HTL processing.

1.8.3 Pressure.

The primary advantage of HTL processing is that energy intensive liquid-to-gas phase changes are avoided by pressurizing the reaction vessel above the saturation vapor pressure of water at a given temperature. Figure 3 outlines the saturation vapor pressure gradient in the subcritical (< 374 °C) region. Operating an HTL vessel above that gradient ensures no endothermic phase changes will occur. Pressure also plays a role at moderating the solvent density within the reaction media. The dense nature of water in the subcritical region aides in uniform biomass decomposition and extraction.

Increasing the operating pressure well beyond the necessary saturation vapor pressure can have deleterious effects on the bio-oil yields. Excessively high local solvent densities can induce a large *solvent cage effect* thereby reducing biomass depolymerization and reformation (Akhtar & Amin, 2011). This effect becomes prominent when moderate temperatures and extreme pressures are employed. The solvent cage affect reduces overall bio-oil yield in two ways:

1) High local solvent density encourages rapid bond recombination after dissociation which often results in daughter fragmentation products recombining to reform the parent molecule.
2) Once reactive species are formed, the dense solvent media can stabilize them and inhibit repolymerization into bio-oil products resulting in increased organic products within the aqueous phase (Akhtar & Amin, 2011).

Thus, HTL systems should be operated at conditions slightly above the required saturation vapor pressure of water under specific temperature regimes. This ensures maximum thermodynamic efficiency while minimizing the deleterious effects of potential solvent cage effects.

1.8.4 Residence Time.

Residence time can play a major role in optimizing bio-oil quantity and quality. In general, longer resides times have been shown to decrease overall bio-oil yields except for cases where very high biomass-to-water ratios were studied (Akhtar & Amin, 2011). Increased residence times are often required to compensate for relatively low conversion temperatures (150 °C) while shorter residence times yield more bio-oil under higher temperature (250-280 °C) profiles (Karagoz S. , Bhaskar, Muta, Sakata, & Azhar, 2004). Bio-oil components have the chance for second and tertiary reactions which can increase the liquid, gas or residue phases; therefore once biomass decomposition has reached its saturation point it is essential to quench the reaction to minimize bio-oil losses (Akhtar & Amin, 2011).

Residence times can also influence the final bio-oil quality from an HTL system. Various residence times studied over two discrete temperature profiles of 180 and 250 °C indicated that reaction products were significantly different (Karagoz S. , Bhaskar, Muta, Sakata, & Azhar, 2004). In addition, longer reaction times where shown to significantly increase the degradation of asphaltenes into lighter products which increased aqueous organic and gas phase products (Boocock & Sherman, 2009). Residence times that maximize the saturation of bio-oil within the HTL media will result in optimal bio-oil yields. Longer residence times will likely encourage increased gas and char products. Selection and identification of the optimum residence time is limited by the relatively

slow heating rates induced by the thick walls of HTL reaction vessels. Most often, longer residence times are necessary to compensate for the limited thermal properties of individual HTL reactors. Many researchers suspect that, like flash pyrolysis, short residence times can increase bio-oil yields by reducing the probably of secondary char forming reactions.

1.8.5 Process Gas and Hydrogen Donors.

Processing gases are employed to stabilize fragmentation products during hydrothermal liquefaction. Char formation can be greatly reduced as reducing species bind with reactive radical products, thus minimizing the amount of condensation, cyclization and repolymerization products which predominantly lead to residue formation (Akhtar & Amin, 2011). Hydrogen gas is often successfully employed in this role; however, its relatively high cost prohibits its long-term use. Yin et al. (2010) published a study which elucidated the role of various processing gases under different temperature profiles during cattle manure HTL processing.

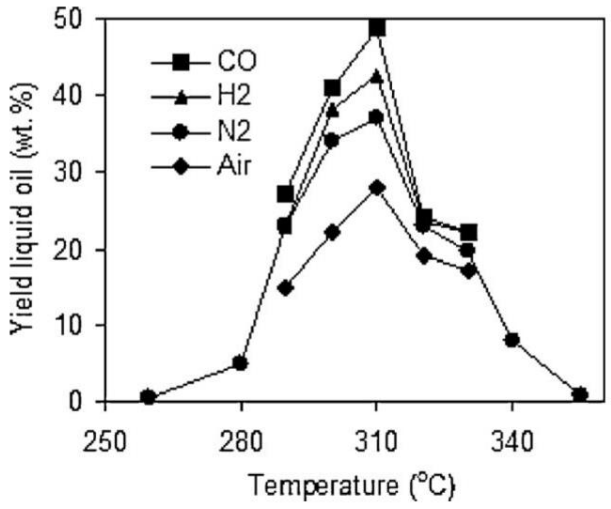

Figure 5. Bio-oil yields from various process gases under similar hydrothermal conditions over various temperature profiles (Yin, Dolan, Harris, & Tan, 2010).

According to figure 5 bio-oil yields peaked around 310 °C indicating that temperature had a greater effect on over yield than the process gas. However, significant improvements can be seen when reducing hydrogen and carbon monoxide gases where

used over inert (N_2) or oxidizing (air) gases. The higher reactivity of hydrogen and carbon monoxide helped stabilize fragmentation products better than inert gases. Air, under all temperature profiles, resulted in decreased bio-oil yields likely due to partial biomass oxidation. Given this observation it is important that non-oxidizing gases be employed during HTL processing to maximize bio-oil production.

Process gases tend to be difficult to introduce into HTL reactor. Additionally, gas channeling and poor distribution within the subcritical media can significantly limit their effectiveness. To combat these issues researchers are exploring the use of hydrogen donor solvents which can provide hydrogen and also act a hydrogen transport vehicle (Wang, Li, Li, & Chen, 2007). The use of tetralin, a common hydrogen donor solvent, increased bio-oil yields of sawdust to 58.9%, a noticeable increase over the baseline 42% using H_2 as a process gas alone (Wang, Li, Li, & Chen, 2007). The improvement of bio-oil yield is likely attributed to the increase in hydrogen accessibly to suppress asphaltene condensation (Akhtar & Amin, 2011). Additionally, hydrogen donating solvents can donate hydrogen to heteroatoms such as oxygen which can combine and form water. By removing oxygen species through water, the heating value and quality of the final oil product can be dramatically increased (Li, Yuan, Zeng, Tong, & Yan, 2009).

1.8.5 Catalysts.

The use of catalysts during HTL processing can greatly enhance bio-oil yields and quality. Homogeneous and heterogeneous catalysts have impressively shown increased performance at reducing char formation by aiding in biomass depolymerization and stabilizing reactive intermediates. Table 3 outlines the catalytic effects of various catalysts during HTL processing.

Catalyst	Feedstock	T (°C)	P (MPa)	Catalytic effect
Na_2CO_3	Corn stalk	276–376	25	Increased oil yield
K_2CO_3	Wood biomass	280	N/A	Less solid residue
Na_2CO_3, Ni	Cellulose	200–350	N/A	Char reduction
K_2CO_3, Ni	Glucose	350	30	Water–gas shift
K_2CO_3	Glucose	400–500	30–50	Water–gas shift
KOH, K_2CO_3	Wet biomass, organic wastes	550–600	25	Water–gas shift
NaOH, KOH, ZrO_2	Stearic acid	400	25	Enhanced decarboxylisation
NaOH, H_2SO_4, TiO_2, ZrO_2	Glucose	200	N/A	Increased isomerization of glucose
Ni	Cellulose	350	18	Enhanced H_2 yield
Ni, Ru	Waste materials	350	21	Enhanced CH_4 yield

Table 3. Summary of various homogeneous and heterogeneous catalysts under HTL conditions (Toor, Rosendahl, & Rudolf, 2011).

Homogeneous catalysts have been used since the advent of HTL processing in the 1940's. E. Berl noted that bio-oil yields were increased under alkaline conditions after adding sodium hydroxide in the reaction media (Berl, 1944). Most homogeneous catalysts researched today are alkali salts which have been shown to accelerate water-gas shift reactions, increase liquid bio-oil yields and improve gasification (Toor, Rosendahl, & Rudolf, 2011). Additionally, the resultant rise in pH increases biomass hydrolysis and also discourages monomer dehydration. Removing excess oxygen in the form of carbon dioxide *decarboxylation* is preferred over water *dehydration* because higher H:C ratios can be achieved in the final bio-oil product.

Alkali additions of the K_2CO_3 used during woody biomass conversion were shown to increase bio-oil yields from 17.8% to 33.7% and reduce residue formation under similar HTL conditions (Karagoz S. , Bhaskar, Muta, & Sakata, 2006). Previous research supporting this observation was conducted a year earlier in which the catalytic activity of different alkali salts was assessed. Potassium catalysts displayed higher activity than their sodium counterparts. Their activity is ranked in the following order: K_2CO_3 > KOH > Na_2CO_3 > NaOH (Karagoz S. , Bhaskar, Muta, Sakata, Oshiki, & Kishimoto, 2005). The carbonate ion is thought to be the primary catalytic driver promoting the gas-shift reaction which results in increased bio-oil yields with higher heating values by promoting the production of H_2 and CO_2 from H_2O and CO. Finally, alkali catalysts have shown enhanced decarboxylation of fatty acids which significantly lowers the oxygen content in the final bio-oil product (Toor, Rosendahl, & Rudolf, 2011).

The utilization of heterogeneous catalysts is limited to low temperature processes where partial gasification of biomass material results in decreased oxygen content. Applications which encounter high-temperatures, such as those in the supercritical region, result in substantial biomass gasification which eliminates bio-oil formation altogether. Few studies have been carried out with the direct intention of improving bio-oil quality or yield with heterogeneous catalysts; however, nickel, palladium and platinum have been shown to increase the quality of HTL gas while not significantly impacting bio-oil yields (Toor, Rosendahl, & Rudolf, 2011). Interested readers can consult an extensive review on the catalytic gasification of biomass under supercritical conditions in a manuscript by Peterson et al. (2008).

Homogeneous and heterogeneous catalysts have found limited utility in large-scale HTL setups. Homogeneous catalysts are difficult to recycle and remove from the product streams while differentiating the effects of supported heterogeneous catalysts from those of nickel-containing stainless steel reactor walls is also difficult. The inactivation and fouling of catalysts' reaction sites is also an important issue. Additionally, alkali salts already present in the biomass feedstocks may act as homogenous catalysts making it difficult to elucidate the true effects of user supplied reagents.

1.9 Degradation of Primary Biomass Constituents.

1.9.1 Carbohydrates.

Biomass contains an abundant amount of polysaccharide material in the form of cellulose, hemicellulose and starch which typically depolymerize into short-chain saccharide and monomeric glucose products under HTL conditions (Toor, Rosendahl, & Rudolf, 2011). Owing to each polymer's chemical and physical properties the degradation rates and final chemical products can vary considerably between different biomass resources. Generally, cellulose is more difficult to break down than hemicellulose and starch because it naturally displays higher degrees of crystallinity than the later. Below the degradation mechanics and resultant products of cellulose, hemicellulose and starch will be examined.

1.9.1.1 Cellulose.

Cellulose exhibits relatively strong intra and inter-molecular hydrogen bonding between β-(1→4) glycosidic linked glucose sub-units resulting in a higher degree of crystallinity (Delmer & Amor, 1995). Under ambient conditions cellulose is insoluble and stable in water and readily resists enzymatic attack; however, under a HTL environment it can be rapidly hydrolyzed into its glucose monomeric sub-units or into semi-stable oligomeic molecules (Peterson, Vogel, R., Froling, Antal, & Tester, 2008). Recent research has shown that the hydrolysis rate of cellulose under HLT conditions (25 MPa) increased nearly 10 times as temperatures increased from 240 to 310 °C (Rogalinski, Liu, Albrecht, & Brunner, 2008). This same study indicated that 100% of the initial cellulose had been degraded within 2 minutes at a temperature of only 280 °C. It was also noted that the glucose decomposition rate was higher than the glucose release rate when temperatures exceeded 250 °C. To improve the cellulose hydrolysis rate, CO_2 was added to increase the carbonic acid content of the media which displayed an acid-catalytic effect on hydrolysis.

Another study performed HTL of microcrystalline cellulose within sub and supercritical (25 MPa and 320-400 °C) conditions. It was found that under subcritical conditions mainly hydrolysis products of monomeric glucose and short chain oligosaccharides were formed. However, under supercritical conditions significant amounts of C3-C6 sugars, aldehydes and furans were detected indicating significant glucose decomposition (Sasaki, Fang, Fukushima, Adschiri, & Arai, 2000). Interestingly, their data suggests that cellulose depolymerization rapidly outpaces monomeric glucose degradation under supercritical conditions. Indeed, short-residence time supercritical hydrothermal processing of cellulosic biomass could prove to be an excellent pretreatment method to hydrolyze cellulose into monomeric sugar units.

1.9.1.2 Hemicellulose.

Depending on biomass type, hemicellulose constitutes roughly 20-40% of plant biomass and also contains a significant proportion of C-5 sugars. Pentose monosaccharides such as xylose and arabinose, as well as hexose units of glucose, galactose and mannose are chiefly found within the plant hemicellulose portion.

Additionally, their lack of uniform structure and relative abundance of side chain units give hemicellulose much lower degrees of polymerization than cellulose (Bobleter O, 1994). Unsurprisingly, hemicellulose is readily solubilized and hydrolyzed into monomeric constituents in water under elevated temperatures of 180 °C. Within 2 minutes nearly all hemicellulosic materials were hydrolyzed into monomeric sub-units under mild HTL (230 °C at 34.5 MPa) conditions (Mok & Antal, 1992).

1.9.1.3 Starch.

Starch, like cellulose, is composed exclusively of glucose linked sub-units; however, their bond linkage is in the form of α-(1→4) which forms a stable helical linear structure called amylose. Additionally, starch can exhibit significant branching from α-(1→6) attachments from its backbone; this form is known as amylopectin and is much less uniform. Like hemicellulose, starches are readily hydrolyzed under HTL conditions. Rapid heating and tight temperature control is essential when studying the hydrolysis and degradation products of starch. Maximum yields of glucose from sweet potato starch were observed at 200-220 °C with 10-30 min residence times. Upping the temperature just 20 degrees to 240 °C severely limited glucose yields as monomeric degradation pathways became dominant (Nagamori & Funazukuri, 2004). Researchers hoping to employ mild HTL to hydrolyze biomass carbohydrates must be conscious of unwanted monomeric degradation products that are also likely to follow, especially in reactors with longer residence times.

1.9.1.4 Glucose.

The six carbon sugar glucose is the predominant monomeric building block of plant carbohydrate biomass. As expected, cellulose, starch and hemicellulose dehydration leads to significant levels of glucose within the HTL media. When dissolved in water, monomeric glucose readily forms open chain, pyranose (6-member) and furanose (5-member) ring structures. Additionally, the open chain form can isomerize to fructose via the *Lobry de Bruyn, Alberda van Ekenstein* reaction which, like glucose, exists in an additional three forms (Toor, Rosendahl, & Rudolf, 2011). An important ramification of this phenomenon is that fructose has been measured to be much more reactive than

glucose under HTL conditions. Complete fructose degradation (~98%) is observed after 2 minutes within HTL media, much higher than reported for glucose (~52%) under identical conditions (Asghari & Yoshida, 2006). Nonetheless recent research has shown that > 90% conversion rates of glucose can be achieved with 1 second reaction times at 350 °C (Kabyemela, Adschiri, Malaluan, & Arai, 1999). The more severe the processing conditions, the less impact the *Lobry de Bruyn, Alberda van Ekenstein* transformation becomes as glucose is quickly degraded.

The rate of isomerization between glucose and fructose is minimal compared to their degradation rates under HTL conditions, thus degradation products can be approximated based on which form the monosaccharide is in. In general, glucose degrades to fragmentation products like: glycolaldehyde, pyruvaldehyde, saccharinic acids, ect (Peterson, Vogel, R., Froling, Antal, & Tester, 2008). Conversely, fructose readily degrades to 5-hydroxymethylfurfural (5-HMF) which can subsequently form phenolic compounds such as 1,2,4-benzenetriol (Luijkx, van Rantwijk, & van Bekkum, 1993). It is no surprise that a wealth of compounds is observed from the conversion of the 6-Carbon monosaccharide portions of biomass; however, by controlling the heating rate researchers can help eliminate side reactions which can substantially increase the amount of expected degradation products. For example, by rapidly heating the biomass components, one can expect rapid polysaccharide dehydration which produces primarily glucose. Because the isomerization of glucose to fructose is slower relative to glucose degradation under HTL conditions, selective degradation of glucose alone can be achieved. Alternatively, slow heating rates can be used to encourage the glucose-to-fructose isomerization resulting in a higher proportion of 5-HMF a promising industrial chemical feedstock.

1.9.1.5 Xylose.

Xylose is a 5-carbon sugar which is found within hemicellulose, it is easily hydrolyzed into the HTL media from hemicellulosic materials. Like glucose it can be found in a pyranose, furanose and open chain forms in water. Xylose finds abundant utility within the chemical sector as a starting material for 2-furaldehyde (furfural) production (Peterson, Vogel, R., Froling, Antal, & Tester, 2008). It has been shown that

the pyranose isomer of xylose readily forms furfural, while the furanose form is relatively stable under mild HTL conditions (Antal Jr, Leesomboon, Mok, & Richards, 1991). This study also showed that the open chain form degrades to a multitude of fragmentation products such as glyceraldehyde, pyruvaldehyde and acetol. Under more extreme HTL conditions furfural can also degrade to similar products as the open chain form of xylose.

1.9.2 Lignin.

Lignin is a complex aromatic heteropolymer component of biomass. P-coumaryl, coniferyl and sinapyl alcohol are its main constituents. Lignin is generally held together by very strong C-C or C-O-C molecular bonds which make the overall macromolecule very stable even under HTL conditions (Toor, Rosendahl, & Rudolf, 2011). Minor degradation products can exist as ether bonds between lignin building blocks are broken. Phenols and methoxy phenols are the most prevalent lignin hydrolysis products. Studies dedicated to lignin conversion via HTL processing have yielded poor results. Often times large residue (char) phases are observed with corresponding small organic molecules in the aqueous phase (Karagoz S. , Bhaskar, Muta, & Sakata, 2005). Unfortunately, no bio-oil fractions are observed when processing biomass with high concentrations of lignin. Because benzene structures are stable under subcritical conditions, some have suggested that supercritical processing would be better suited for high lignin feedstocks such as perennial grasses and woody biomass. Within the supercritical region, radical dominated reactions would likely better fractionate and degrade lignin macromolecules into light gaseous compounds.

1.9.3 Protein.

Many biomass components have high protein contents which could be processed into high value feed, pharmaceuticals or cosmetics. The amino-acid building blocks of plant and animal proteins have a large economic potential, therefore researchers have been interested in low cost processing technologies such as HTL to extract amino acids from animal or biomass resources. To achieve protein depolymerization the peptide bond linking the carboxyl group of one amino acid to the amine group of the second must be split. This C-N bond readily hydrolyzes within HTL media; however, limited amino acids

are recovered because significant residue degradation occurs even under mild HTL processing (Peterson, Vogel, R., Froling, Antal, & Tester, 2008). For this reason limited follow-up studies have been conducted utilizing HTL for amino acid extraction.

1.9.3.1 Amino Acids.

All proteins are constructed of 21 various amino acids which display diverse properties based on the chemical properties of their side chains. All amino acids share a similar peptide backbone and therefore undergo similar decarboxylation and deamination reactions (Toor, Rosendahl, & Rudolf, 2011). A 70% degradation of glycine and alanine was shown to occur under subcritical conditions of 350 °C @ 24-34MPa with a 30 second residence time (Klingler, Berg, & Vogel, 2007). They found simple degradation products of: acetaldehyde, ethylamine, methylamine, formaldehyde, lactic and propionic acids. Significant deamination occurred through ammonia and organic acid production while decarboxylation produced carbonic acid. In general, HTL benefits from extensive deamination and decarboxylation reactions because the resultant bio-oil's composition will have lower N and O contents and have higher H:C ratios. As Toor et al. (2011) points out, the hydrolysis of biomass and proteins together can induce significant Maillard reactions which lead to the formation of N-containing cyclic organic compounds which end up in the bio-oil fraction. Although these reactions can act as free radical scavengers to inhibit char residue condensation, they also increase the N content of the bio-oil fraction, thus reducing its quality.

1.9.4 Lipids.

Lipids, or triacylglycerols (TAGs), are non-polar triesters of fatty acids attached to a glycerol backbone. Given the strong polar nature of water under ambient conditions limited solubility with saturated non-polar TAGs is achieved; however, as shown in figure 4, water's dielectric constant drops off considerably as processing conditions approach the supercritical region. The reduction of water's dielectric constant, reflecting the non-polar solvation power of subcritical water, drastically increases the solubility of non-polar compounds such as biomass TAG's. For this reason HTL processing is uniquely well suited for biomass feedstocks with high fat or oil content. Rapid TAG

hydrolysis, as seen with soybean oil feedstocks, readily takes place within acid free media (King, Holliday, & List, 1999). Hydrolytic efficiency rates of 90-100% are commonly achieved with resultant products taking the form of free fatty acids and glycerol. As with biomass's protein and carbohydrate portions, TAG hydrolysis products can subsequently undergo additional degradation reactions.

1.9.4.1 Glycerol.

As noted above, glycerol is one of the main products produced during TAG hydrolysis. Under HTL conditions glycerol is not stable and often degrades to aqueous phase organics. In fact, studies on pure glycerol yielded no bio-oil compounds. Conversion rates as high as 31% were achieved when glycerol was decomposed under varying HTL conditions. The main products observed were: methanol, acetaldehyde, acrolein, ethanol and formaldehyde with gaseous products of CO, CO_2 and H_2 (Buhler, Dinjus, Ederer, Kruse, & Mas, 2002). Given that HTL processing of glycerol yields no bio-oil products an alternative conversion scheme which separates glycerol before high-temperature treatment might improve the economics of large-scale HTL conversion of fatty and oleaginous feedstocks.

1.9.4.2 Fatty Acids.

In general, free fatty acids are quite stable under HTL conditions. Under uncatalyzed conditions hydrocarbon yields from fatty acids are relatively low, however, when homogeneous catalysts such as KOH are added excellent hydrocarbon yields can be achieved. Conversion of steric acid, a model compound of free fatty acid, can yield up to 32% long-chain hydrocarbons when processed under alkaline HTL (400°C, 25 MPa, 30 min) conditions (Watanabe, Iida, & Inomata, 2006). Unreacted fatty acids still end up in the bio-oil phase and substantially increase its overall heating value. Because free fatty acids and their degradation products ultimately end up in the bio-oil phase, HTL processing of TAG-rich biomass feedstock has received increased attention recently. Given algae's large TAG accumulation potential, many researchers have proposed HTL as the ideal conversion pathway for algal feedstocks.

1.10 Feedstock and Product Interrelatedness.

1.10.1 Feedstock Characteristics.

Hydrothermal liquefaction of organic materials and biomass feedstocks has been well studied in batch autoclave reactors. In general, almost any lignocellulosic, agricultural residue, sewage, animal offal and municipal solid waste feedstock can be processed with HTL technologies. The major limitation to what type of feedstock can be converted lies directly on what the HTL reactor can accommodate. Since most HTL studies are carried out with a batch process, particle size constraints and feedstock viscosity are minimal considerations. Continuous HTL reactors need more scrutiny as their feedstocks must first go through a high-pressure pump and complex pressure regulation systems. In general, particle sizes must be very small (< 1.0mm), the feedstock slurry must have the low viscosity and the particles should be soft in nature. Highly abrasive feedstocks, even when processed down to the micrometer level will significantly degrade delicate sealing faces on high pressure equipment. Typically, continuous HTL reactors are run with waste streams containing 10-20% solids while batch reactors can accommodate much higher solids concentration.

Feedstock slurries with the consistency of toothpaste are ideal for continuous processes; however, biomass pretreatment costs to achieve that consistency should be kept to a minimum. Wood chips and grassy feedstocks are more readily processed in batch reactors. In fact, lignocellulosic woody residues likely find more utility for pyrolytic conversion because the cost to drive out the remaining water in those biomass resources is much lower than compared to sludge-like or slurried biomass feedstocks.

1.10.2 Feedstock Heterogeneity and Product Yields.

Given the vast heterogeneity of biomass constituents and the varied chemical compositions of diverse waste streams it is no surprise that HTL products can vary significantly in quality and quantity. Subcritical processing of biomass typically yields a bio-oil, aqueous organic and gaseous phase; section 1.7 provides an overview of relevant details for these phases. The physical properties of each phase strongly correlate to the parent feedstock's physicochemical characteristics. For example, bio-oils derived from

Substrate	Conditions	Oil properties
Swine manure	285–305 °C 5.5–18 MPa 5–180 min CO as red. agent	Yield: 61% (on total solids) Heating value: 35 MJ/kg Composition: C: 71%, H: 8.9%, N: 4.1%, O: 14.2%, and S: 0.21 ppm
Garbage	340 °C 18 MPa 0.5 h Na_2CO_3 as catalyst	Yield: 21% (on total solids) Heating value: 36 MJ/kg Composition: C: 73.6%, H: 9.1%, N: 4.6%, O: 12.7%.
Indonesian biomass residues	300 °C 10 MPa 30 min Na_2CO_3 as catalyst	Yields between 21 and 36% (on total organics) Heating value: ≈30 MJ/kg Composition: C: 67–80%, H: 6–8%, N: 0–2%, O: 11–23%
Sawdust, rice husk lignin and cellulose	280 °C 15 min	Yields were ~8%
Algae *Dunaliella tertiolecta*	360 °C 50 min 5% Na_2CO_3	Yield: 25.8% Heating value: 30.7 MJ/kg C: 63.55%, H: 7.66%, N: 3.71%, O: 25.08%
Chlorella, Nannochloropsis, Porphyridium and Spirulina	350 °C 20 MPa 1 h 1 M Na_2CO_3 1 M formic acid or pure distilled Water	Yields: 5–25% Heating values: 22.8–36.9 MJ/kg C: 66–83%, H: 5–11%, N: 0–11.9%, O: 8–27% and S: 0–1%.

Table 4. Summary of bio-oil yield and quality from various feedstocks under similar HTL conditions (Toor, Rosendahl, & Rudolf, 2011).

high protein feedstocks such as animal offal or microalgae often contain much higher levels of Nitrogen and Sulfur than their low protein woody biomass cousins. Additionally, lignocellulosic materials often yield much less bio-oil than highly fat or lipid containing wastes. Table 4 summarizes the resultant bio-oil properties from various feedstocks under similar processing conditions. Note the variation in bio-oil yields while chemical compositions are relatively stable. Most feedstocks processed resulted in bio-oil HHV's of 30-37 MJ kg^{-1} indicating that upgrading of the biomass has indeed taken place.

An interesting study carried out by researchers from the University of Illinois helped elucidate the interrelatedness of initial feedstock physiochemical characteristics

and final product compositions. The batch processing of *Spirulina* algae, swine manure and anaerobic sludge were carried in a 2.0 L Parr 4500 reactor fitted with an electric heater, magnetic stirrer and gas injection ports. They adjusted 800 g of feedstock slurry to 20% solids (w/w). The reaction was carried out at 300 °C with a 30 minute residence time. Prior analysis of initial feedstock protein, lipid, lignin and ash content was compared to the final bio-oil yield and quality. After conversion it was found that oil yields of 32.6, 30.2 and 9.4% (with HHV's of 33.2, 34.7 and 32.0 MJ kg^{-1}) were obtained from *Spirulina*, swine manure and anaerobic sludge respectively (Vardon, et al., 2011). Final C:H:N:O:S bio-oil composition ratios ranged from 66.6-71.2 : 8.9-9.5 : 3.7-6.5 : 14.9-18.9 : 0.12-0.97 respectively. These ratios are comparable to those reported in table 4 of other biomass resources. Interestingly, they observed that much of *Spirulina's* initial high protein content can be successfully converted into bio-oil with a good heating value and minimal nitrogen content. This result contrasted against their expected result of increased bio-oil yields from swine manure due to its high initial lipid content compared to *Spirulina*.

It is generally accepted that HLT conversion efficiency follows the trend: lipids > protein > carbohydrates (Biller & Ross, 2011). Given Vardon et al's results HTL conversion of high protein content feedstocks can yield similar bio-oil yields as their high-lipid counterparts. This is a significant observation because often times the productivity of high-protein microorganisms can be significantly higher than their high lipid counterparts. Large-scale bio-energy crop production systems can be more readily managed knowing that biochemically dissimilar feedstocks can be easily converted to comparable bio-oils, without significant yield or quality losses.

Vardon et al, also noted that no straight chain hydrocarbons were identified in the final bio-oil reflecting the enormous chemical complexity of the final product. Furthermore, they "emphasize the need for feedstock characterization and selection based on the intended downstream application." Even though each feedstock yielded similar elemental distributions their unique chemical makeup, specifically their heteroatom contents, primarily N and O, resulted in vastly different bio-oils suited for diverse applications. Although HTL processing can be done on a variety of feedstocks, its

conversion limitations and resultant product characteristics should be carefully assessed before large investments are made.

1.10.3 HTL Conversion of Microalgal Feedstocks.

Biller et al. (2011) studied 3.0 g samples of four different microalgal strains ranging from high protein to high lipid content under identical HTL (350 °C for 1 hour) conditions. They confirmed that the bio-oil production is an additive process meaning initial feedstock biochemical composition highly predicts the maximum attainable bio-oil yields. The resultant model was derived:

$$\begin{aligned} &Biocrude\ yield\ \% \\ &\quad = (Protein\ yield\ \% * Protein\ content\ \%) \\ &\quad + (Carbohydrate\ yield\ \% * Carbohydrate\ content\ \%) \\ &\quad + (Lipid\ yield\ \% * Lipid\ content\ \%) \end{aligned}$$

Equation 3. Bio-Crude yield based on initial feedstock composition (Biller & Ross, 2011).

After assessing the bio-oil yields from various model compounds, Biller et al. estimated that 11-18%, 6-16% and 55-80% of the initial protein, carbohydrate and lipid portions respectively are successfully converted to bio-oil. By analyzing the synergistic effects of 1M formic acid (employed as a reducing agent), and 1M Na_2CO_3 (an alkali catalyst) they were able tease out the optimal conversion conditions for each feedstock. It was found that high lipid and protein algae are best processed in water or slightly reducing environments while alkali catalysts yielded more bio-oil for high carbohydrate algal strains (Biller & Ross, 2011). Each algal strain produced a bio-oil yield that agreed well with the above model. Resultant bio-oils displayed HHV's between 33-39 MJ kg^{-1} which is in agreement with previous studies. As expected, high lipid algae produced the higher quality bio-oils, while high protein algae yielded increased N levels in the oil fraction.

Any analysis of the energy efficiency of processing each microalgae strain was also conducted. The energy recovery ratio (EERs) is defined as:

$$EER(\%) = \frac{(HHV\ of\ biocrude\ *\ mass\ of\ biocrude)]}{(HHV\ of\ feed\ *\ mass\ of\ feed)} * 100\%$$

Equation 4. Energy Recovery Ratio (Biller & Ross, 2011).

EERs ranged from 19.3-66.1% depending on operational parameters. The highest EER was observed with high lipid algae converted without catalytic additions, while high protein strains yielded the least favorable results (Biller & Ross, 2011). An analysis of the energy required to dry wet algal paste compared with the energy released upon combustion showed an unfavorable energy balance indicating microalgae are poor candidates for direct combustion or co-firing applications. Conversely, HTL processing of microalgae yields 1 to 2 times the amount of bio-crude energy as the amount of process energy input needed to heat the slurry. Herein lies the inherent advantages of HTL processing, by eliminating the energetic losses due to vaporization considerable energy savings can be achieved. Collecting and utilizing the heating content within the aqueous organic and/or gas phases could dramatically enhance reported HTL energy recovery and utilization figures.

1.11 Enhancing HTL Processing.

1.11.1 Batch Process Limitations.

As noted earlier an extensive amount of HTL research has been carried out using lab and bench-scale batch autoclave reactors. Assessing the long-term viability and industrial scale-up potential of various biomass resources requires a flexible and robust continuous conversion process that can help overcome the significant batch processing limitations which include the following:

- Poor thermal transfer.
- Excessively long heat-up and cool-down times.
- Limited heat recovery potential.
- Poor process control.
- Limited feedstock loading and conversion product output.
- Product separation and extraction difficultly.

Continuous HTL processing allows for greater operator control over the necessary parameters including conversion temperature, reaction pressure, flow-rate (residence

time) and product separation and extraction. Additionally, transforming batch HTL into a continuous process allows for heat recovery and in-situ product analysis which can greatly aide energy and technical feasibility studies. Feedstock handling imposes some pretreatment steps, mainly blending and maceration, to ensure biomass particles are compatible with sensitive high-pressure pump and flow control systems (Ocfemia, Zhang, & Funk, 2006). Therefore, it is important to consider what types of biomass and/or organic feedstocks are conducive to continuous processing. Highly abrasive or viscous feedstocks require more pretreatment which can significantly limit their long-term economic viability.

1.11.2 Continuous HTL Development.

Researchers from the University of Illinois at Urbana Champaign (UIUC) began development of a continuous hydrothermal processing reactor specifically tailored for swine manure in 2005. They outfitted their reaction system with a valveless rotary piston pump to achieve the high pressure slurries necessary for their process. A modified 2.0 L continuously stirred reactor was employed for the hydro-processing vessel because as previous experience with screw-type plug flow reactors resulted in significant clogging. An additional smaller 1.8 L stirred vessel was used for facilitating product separation; significant stirring was used to achieve homogenous conditions which reduced solids build up within the system. A ball and needle valve were used in series as the pressure let down device. Figure 6, found below, details their final system. Tertiary system components such as flow and process controllers are also noted.

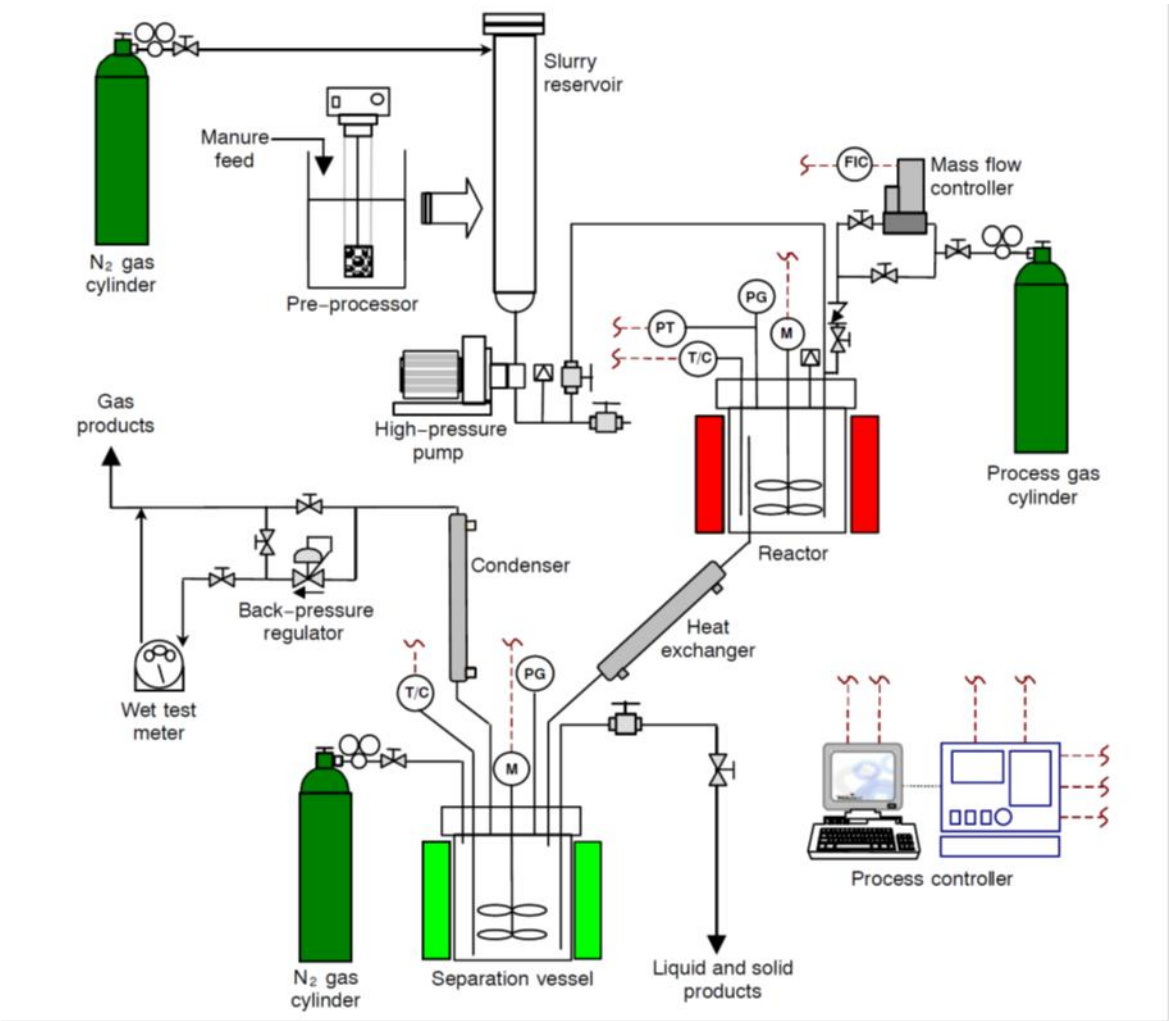

Figure 6. Detailed schematic of University of Illinois continuous hydrothermal process reactor system (Ocfemia, Zhang, & Funk, 2006).

Ocfemia et al., from UIUC, were able to run their system for up to 16 hours at a time before either system clogging interrupted the slurry flow rate or abrasive feedstock particles eroded the valveless pump's delicate sealing surfaces. In a follow-up study they were able to test various HTL conditions for optimal bio-oil production from swine manure. Temperatures from 285-305 °C, pressures from 9.0-12.1 MPa, residence times from 40-80 minutes and the impact of CO as a processing gas were explored. Three dimensional surface plots were used to analyze the data; optimal bio-oil production conditions were found to be 300 °C and 10.5 MPa regardless of residence times studied while addition of CO increased bio-oil quality (Ocfemia, Zhang, & Funk, 2006). The flexibility of UIUC's continuous processing system provides, especially for identifying

ideal conversion parameters and economic viability, has served as a solid model for the development of future HTL systems tailored for additional feedstocks.

1.11.3 Previous UMN Research and Development Efforts.

Research carried out at the University of Minnesota's Center for Biorefining aimed at producing a continuous plug-flow style hydrothermal processing reactor with the capability of reaching supercritical conditions. A screw-type gear pump was initially sought for pumping the slurry to high pressure; unfortunately, the corn-cob feedstock tested resulted in poor pump high pressure performance. Eventually an air driven piston diaphragm pump was identified that could pump macerated slurries to high pressures (27.6 MPa). After careful consideration, a Techne fluidized sand bath capable of reaching 600 °C was employed for heating. The primary hydrothermal processing reactor consisted of a serpentine ~25 foot length of stainless steel tubing (0.50 in OD, 0.37 in ID) immersed in the sand bath.

Many processing issues were noted; of the most important, flow rate control, pressure pulsation and increasing the slurry heating rate were identified as the most significant. To achieve the set point temperature of ~325 °C significant pre-heating was required to assist the Techne sand bath in achieving stable slurry temperatures. Additionally, minimal process flow rates of < 30ml min^{-1} were attainable due to the limited heating capacity of processing reactor. Overall recommendations for improving the process were made, they are listed below:

1. Increase heating rate to allow higher throughput.
2. Increase heat recovery and recycling.
3. Reduce length of tubing required for the processing reactor.
4. Eliminate problematic char/tar accumulation spots.
5. Improve high-pressure regulation, reduce pump pulsation.
6. Modify back-pressure regulation.
7. Supply attachment(s) for fixed bed catalysts.
8. Reduce laboratory footprint of hydro-processing reactor.

Previous researchers have also suggested focusing on a specific targeted feedstock. By specifically tailoring for one feedstock, some of the above issues become less pronounced. Following sections of this narrative will outline our group's continuing effort to overcome the substantial technical barriers of developing a continuous

hydrothermal processing system. By re-designing and outfitting our next generation hydrothermal processing system, we hope to overcome the significant technological barriers of scaling up hydrothermal liquefaction technologies for the conversion of promising biomass feedstocks.

PROBLEM STATEMENT

2.1 Scope and R&D Opportunities.

2.1.1 Scope of Project.

Recent attempts at constructing a scalable continuous hydrothermal liquefaction (CHTL) conversion system have been met with limited success. The primary goal of this project is to identify and overcome the technical and economic barriers that impede further development and the large-scale deployment of promising HTL technologies. Using knowledge gained and lessons learned from section 1.11, our research team aims to develop a new CHTL system specifically catered for aqueous microalgae biomass feedstocks.

2.1.2 Major CHTL Issues and Research Justifications.

To date, the limited success of CHTL technologies can be primarily attributed to poor thermal heat transfer from the heating source to the reaction media resulting in longer heat up and cool down times. This not only increases the biomass to bio-oil conversion time, but also has additional deleterious effects. Slow heating rates and long residence times can result in significant bio-oil yield reductions through the promotion of secondary and tertiary condensation reactions resulting in excess char and tar formation which complicate system operation by coating or clogging sensitive components. In attempts to overcome poor thermal transfer, researchers have employed progressively larger heating sources or modified the hydrothermal processing reactors in hopes to mitigate this issue. Although improvements have been observed, significant processing issues remain in further reducing reactor complexity and minimizing the potential for clogging. Addressing the poor thermal transfer rates of conventional batch and continuous hydrothermal processing systems is at the core of our projects' objective.

A successful CHTL system will integrate a wide range of reactor tuning options. As noted from section 1.8, there are many other important factors that affect the overall yield and conversion efficiency of the HTL conversion process. Allowing the user the ability to tune the reactor conditions for specific feedstocks, or for maximizing product yields, will allow for greater system flexibility and robust operation. Feedstock slurry pressure and flow rate control have been identified as the most important factors outside of heating that need the most improvement for the continuous system. Including the capability to accommodate process gases and/or catalysts throughout the system is also beneficial. Because initial biomass feedstock characteristics also dictate the ideal conversion environment, the CHTL system must incorporate precise and accurate parameter control based on user input, the automation of such parameters is preferred.

2.1.3 Algal Biomass Conversion.

Algae-based bio-energy crop production systems are still in their infancy. Although many best management practices have helped reduce the costs of growing algae at scale, the high costs of harvesting and down-stream conversion barriers have severely limited algae-based materials and fuels from reaching market parity with their petroleum counterparts. Avoiding the energy-intensive step of drying harvested algal paste will significantly improve the economics of large-scale production systems. Furthermore, pursing a robust conversion process that can utilize the entire algal cell, not just its starch or lipid components, would greatly simplify the utilization of this promising feedstock. Although algae shows promising potential in helping early adopters achieve energy security, it remains to be seen how economical and practical current biochemical and thermochemical conversion platforms are at scale.

2.2 Synergistic Opportunities.

2.2.1 CHTL Platform for Algal Slurry Conversion.

Given the challenges outlined above, our thermochemical conversion and algae-production groups feel that there is a significant synergistic opportunity present by coupling continuous hydrothermal liquefaction technologies with an algal production system. By specifically designing a CHTL system to accommodate wet algal pastes we

believe significant technical and economic barriers can be overcome in the algae-to-biofuels logistical chain. Utilizing wet algal pastes allows the algal-crop producer to focus on maximizing algae productivity without worrying about the high costs of harvesting and drying. During conventional algae energy crop culture, rapid mixing is often employed within the photobioreactor to overcome natural flocculation, or self-settling, of algal cells. By utilizing algal pastes directly significant reductions in energy inputs needed for mixing and harvesting can be achieved. Fortuitously, harvested algal pastes display ideal physical characteristics for direct HLT conversion such as; ~15% (w/w) solids ratio, pump-able viscosity ranges, and they are composed of non-abrasive soft organic particles.

Rapid heating of the algal slurry during HTL can be achieved with ohmic heating which significantly reduces processing costs and can potentially increase bio-oil yields. Because algae lack complex biopolymers such as lignin they are uniquely suited for continuous hydrothermal processing; reduced amounts of char and tar accumulation can be expected for low lignin feedstocks. HTL processing of algae can also utilize the entire cell without introducing prohibitive extraction costs. Previous HTL batch experiments of microalgae have shown that their intracellular components of cellulose, starch, protein and lipid can be successful converted to bio-oil. By engineering an advanced CHTL system to accommodate algal paste conversion to bio-oil this project aims to improve the efficacy of the entire algae-to-biofuels pathway.

OBJECTIVES

3.1 Improve Heating Rate Performance.

3.1.1 The Ohmic Heating Advantage.

Direct ohmic heating of liquid slurries has increasingly found utility in the food processing industry as an efficient, fast and uniform heating process. Ohmic heating involves passing an electric current though the slurry; as electrons travel from the power source to ground, the electrical resistance of the media results in the rapid heating of the substrate. Because ohmic heating results in raising the temperature of the slurry from the

inside-out considerable benefits are observed over conventional outside-in heating processes. Biomass particles contained within the slurry media heat quickly and uniformly as the electric current rises the nearby solvent temperature. Ohmic heating also overcomes the considerable heat transfer limitations imposed by conventional heating methods. By eliminating the relatively slow heat transfer rates imposed by thick stainless steel reactor walls much higher slurry heating rates can be achieved.

The rate of slurry heating, per *Joule's 1st Law* is directly proportional to the square of the current passed through it and its electrical resistance for a specific time period. Since the resistance of the slurry remains fairly constant simply varying the time or current (which is dependent on the voltage potential between the two electrodes) is all that is necessary to operate a simple ohmic heating device. Ionic salts such as sodium chloride can also be used to condition the slurry to the proper conductivity for optimal ohmic heating. Additionally, the direct conversion of electrical current to thermal energy results in efficient electrical energy utilization rates in excess of 90% (Ruan, Ye, Chen, Doona, & Taub, 2001).

Given the tremendous benefits and flexibility offered by direct ohmic heating, our group aims to engineer an ohmic heating device capable of operating within the sub-critical HTL region. To our knowledge no published attempts have been made to outfit a hydrothermal liquefaction system with a direct ohmic heating device. Since harvested algal pastes already contain a large amount to ionic material little to no ionic conditioning will be necessary, thus simplifying HTL pre-treatment steps. The real challenge of employing direct ohmic heating within the subcritical region is engineering a heating apparatus capable of sustained operation under high temperature (300-400 °C) and high pressure (14-28 MPa) regimes without mechanical failures or electrical faults. Many ohmic heating devices have been successfully engineered and operated at much more moderate temperature regimes of (60-150 °C) where dielectric materials such as Teflon (PTFE) can be easily employed without worry of mechanical failure. Additionally, achieving a hermetic air-tight seal under subcritical conditions is no small task. Indeed, intuitive design and proper material selection will be paramount to the successful marriage of direct slurry ohmic heating technologies and the extreme environmental conditions of HTL processing.

3.2 Periphery Improvement.

3.2.1 Pressure Regulation.

Improving the pressure regulation components of the HTL system was identified as a central priority to enhancing the overall performance of the CHTL process. Prior attempts at precise pressure regulation were met with challenges. Char and tar accumulation would periodically block or stick to sensitive components. Additionally, common industrial spring-driven regulators were found to be incompatible with the post-HTL slurry product streams. Prior experience using a ball and needle valve in series proved to moderate system pressure; however, this setup is far from ideal for a continuous operation. We suspect that automated stem or diaphragm regulators might serve this function well in the redesigned system.

Flow rate and slurry residence times are delicately linked to the pressure control system. Increasing the pressure gradient from inlet to outlet will increase the flow rate and result in decreased residence times. Given the immense variation of ideal residence times for processing various biomass resources in previously published batch HTL studies, we identified the need to allow user control of this important parameter. The best way to accomplish this goal is to incorporate precise and accurate inflow and outflow pressure regulation of the continuous system. In this way the end user can achieve a desired residence time by tuning the pressure gradient from inlet to outlet. Identifying the types of inlet and outlet pressure control devices capable of accommodating very small flow rates and the special properties of each stream will need to be addressed.

3.2.2 Hybrid Reactor Design.

The hydrothermal reactor is arguably the most important component of any HTL system; this is where the high-temperature decomposition and reformation of biomass takes place. Typical batch processing employs a sealed stainless autoclave which is heated from the outside-in by a resistance wire heater connected to an external temperature controller. The autoclave is typically outfitted with a built-in mixer with inlet and outlet ports for process gas additions and safety components. A reactor of this type is typically referred to a continuously-stirred tank reactor (CSTR). A CSTR can also be

modified for continuous use by incorporating additional slurry inlet and outlet ports. In this way, fresh biomass slurries can be simultaneously mixed with intermediate HTL reaction products in the reactor. This type of reactor is typically preferred given its proven safety track record and ease of use. Unfortunately, CHTL systems employing this type of reactor are often plagued with requiring small slurry flow rates resulting in long residence times. CSTR vessels are limited in their heat transfer and slurry heating rates based on the size of their heating apparatus and the thick stainless steel walls of reactor. To overcome these limitations longer residence times or lower flow rates are often needed to achieve very high temperatures. Unfortunately, these conditions also increase the probability of char production and significantly decrease the throughput of the CHTL system.

Another type of popular hydrothermal processing vessel is the plug-flow reactor. This type is reactor is simply a tube in which the slurry is pumped through, some type of external heat source again supplies thermal energy. A major benefit of this type of reactor is greater temperature control and the ability to achieve higher heating rates due to an increased tubing surface area and thinner reactor walls. Previous attempts at engineering a plug-flow reactor in our lab utilized T316 SS tubing (0.50 OD, 0.37 in ID) in a serpentine arrangement that was submerged in a high temperature fluidized sand bath. Ideally, the slurry media's velocity would remain constant throughout the cross-sectional profile of the tubing; however, this is often not a reality. Under low flow rates (laminar conditions) the slurry experiences frictional drag forces that slow the media near the internal tubing surface. This often leads to excessive heating and slurry charring on the tubing walls with unreacted material in the center, as time progresses this phenomenon becomes increasingly problematic. To achieve very high processing temperatures (> 350 °C) very long sections of tubing must be employed which further increase reactor complexity and material costs.

Although CSTR and plug-flow reactors have been employed in CHTL applications, we seek to improve their benefits by integrating concepts from both into a hybrid design. By incorporating an ohmic heating device upstream of the CSTR vessel we hope to achieve very high heating rates of the biomass slurry while maximizing the benefits of CSTR vessels. Because upstream pre-heating has taken place, the heating

requirement of the CSTR vessel will be reduced to simply maintaining the reaction temperature. In-stream direct ohmic heating, while mimicking a plug-flow type environment, will require a fraction of the materials to achieve the same effect. Additionally, heating the slurry stream from the inside-out should significantly decrease the charring potential of the system. By employing an ohmic heating apparatus as a pre-heater upstream from the CSTR, very high heating rates and system throughputs can be achieved while providing the synergistic beneficial assets of combining continuously-stirred and plug-flow type reactors in a sequential arrangement.

METHODOLGY AND DESIGN PROTOTYPES

4.1 CHTL System Overview.

4.1.1 Research Agenda and Basic System Layout.

The continuous hydrothermal liquefaction system developed under this work aims to provide a wide variety of operational control and system reliability in an easily scalable design. The primarily targeted feedstock for this study is harvested algal paste which is ~15% solids (w/w) and is composed of *soft* non-abrasive particles. This paste will be collected from a pilot-scale algal biomass production site located at UMORE Park in Rosemount, MN. The algal strain cultivated is a *Chlorella sp.* displaying high lipid productivity when grown within animal waste streams. Ideally our CHTL system will accommodate a range of liquid biomass slurries; however, the high potential of algal biomass coupled with our group's extensive knowledge of its large-scale cultivation makes it our priority candidate for this study.

Given the operating parameters of previously published reports on the batch processing of various algal biomass feedstocks, our objective is to develop a CHTL system with a nominal operating range of 200-400 °C and 6-28 MPa effectively allowing a range of sub and supercritical operating conditions. Additionally, we aim to provide process gas and heterogeneous catalysts accommodations for future liquefaction studies. Much knowledge and operational insight has been gained from previous attempts at producing a fully functional reliable CHTL system. In fact, the basic structural

components from one design to the next must be upheld. Because the system operates under pressure and needs to be continuous, a high pressure fluid pump must be employed. Additionally, pressure and temperature management components must be built into the system. Although some components such as pumps, regulators, heaters and tubing are standard for all CHTL systems; their arrangement, function or management can vary widely from one design to the next. Hence, each CHTL system is unique in its own right. By targeting algal biomass and incorporating a fast ohmic heating device we strive to produce the first industrially scalable and economical liquefaction platform to date.

4.1.2 Description of Components.

The CHTL system constructed is composed of eleven primary components. Figure 7 outlines a simplified process flow diagram of the system. A host of periphery safely and monitoring components are also employed. All critical components are mounted to a cart which is encased with Plexiglas for added laboratory mobility and safety. A pane of ballistics glass is used to shield the operator as a redundant safety precaution. Descriptions and rationalizations for the eleven major components listed in figure 7 are outlined below.

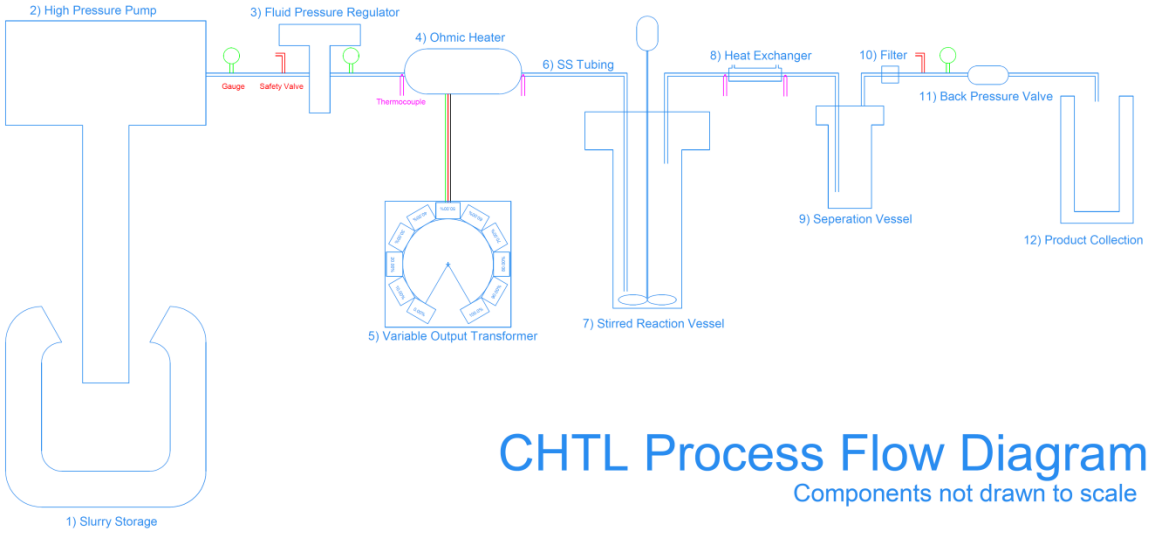

Figure 7. UMN CHTL Process Flow Diagram. Image provided by Michael Mohr.

1. Slurry Storage: A simple bucket can be used for slurry storage. The high pressure pump draws the slurry from bucket and into the CHTL system. For this research a 5 Gallon *Menards* pail was used to hold the slurry feedstock.

2. High Pressure Pump: *Graco Merkur Piston Pump* (Model #040.035) with max flow rate of 16.2 L min^{-1} and max operating pressure 27.6 MPa is employed. This positive displacement dual check valve piston pump is proportionally driven by an external 0.00-0.69 MPa (0-100 psi) air pressure source. The *Merkur* line of piston pumps was originally developed for airless spraying technologies where the end user could apply viscous liquids such as paints or lacquers without a carrying solvent. Fortunately, this type of pump works very well at accommodating soft organic slurries such at algal pastes. Biomass slurries with abrasive particle rapidly deteriorate delicate check valve sealing surfaces inhibiting the pumps ability to build pressure.

3. Fluid Pressure Regulator: Although the output of the high pressure pump can accommodate a range of operating conditions, pump strokes needed to build pressure would significantly disrupt the pressure set point of the system. To alleviate the pump hammering effect a *Graco* high pressure fluid regulator (Model #238894) was employed to regulate the high pressure source down to the operating set point. Like the Merkur pump, this regulator is also proportionally driven by an external 0.00-0.69 MPa compressed air source. It can regulate a 41.4 MPa inlet source down to a range of 3.44-27.6 MPa. By using the high pressure regulator in conjunction with the piston pump, greater inlet pressure control accuracy can be achieved while minimizing the hammering effect from the piston pump.

4. Ohmic Heater: This item's concept of operation and development will be outlined in following sections. The primary function of the device is to pre-heat the algal slurry via direct ohmic heating very rapidly under sub or supercritical conditions. Thus, it is imperative that this device be capable of continuous operating conditions of 27.6 MPa at 400 °C.

5. Variable Output Transformer: This component's role is to provide a steady single phase alternating current source for the ohmic heating device. A manually driven *Staco Energy Products Co* (Model# 5021CT) transformer was identified as an ideal candidate. This model has accepts an input voltage of 120VAC and provides a variable output of 0-280 VAC with a 28 Ampere rating.

6. Stainless Steel Tubing: Seamless Stainless Steel T316 tubing from *Swagelok* (SS-T8-S-065-20) with an outside diameter of 0.50 in and nominal thickness of 0.065 in was chosen to connect the various components of the CHTL system. This tubing dimension afforded the greatest flexibility in fitting connections while not compromising strength at temperature. Under normal operating conditions (-17.8 - 43.3 °C) this tubing is rate at 35.2 MPa. Swagelok suggests a de-rating factor of 0.79 to be applied when operating the tubing at 426 °C. This yields an operating pressure of 27.8 MPa which is ideal for our system's maximum target pressure and temperature ranges.

7. Stirred Reaction Vessel: A bench top reactor rated to 34.5 MPa @ 500 °C from *Parr Instruments* (Model# 4575) equipped with stirring device was selected as the primary vessel for the CHTL system. The 0.50 L reactor is outfitted with an automated temperature controller and variable rpm controller. Here freshly heated slurry comes into contact with intermediate products and undergoes the decomposition and reformation reactions characteristic of hydrothermal liquefaction.

8. Heat Exchanger: A custom engineered (~12 in) cross flow heat exchanger utilizing 0.50 and 1.00 in OD *Swagelok* tubing is used to quench the liquefaction reaction to room temperature using tap water as the heat transfer fluid. Cooling the reaction is important for two major reasons; the first involves stopping intermediate condensation reactions which might produce unwanted char or tar products from the bio-oil fraction. The second is to cool the reaction media to a temperature below the allowable limits for sensitive downstream components.

9. Separation Vessel: The goal of this vessel is gravity clarification of the reaction media. Denser organic char/tar residues passively settle to the bottom while the lighter gaseous, aqueous and oil phase products exit through the top. A modified 2.0L *Parr* reactor (Model# NS18064C3 T316 10050 33634) rated for 34.5 MPa @ 500 °C with dip tubes is employed for this function. In-situ char removal is difficult; as the separation vessel fills with solids the CHTL must be shut down to remove the accumulated char residues.

10. Filter: A 140 µm pore size filter from *Swagelok* (Model # SS-4TF4-140) is utilized to protect downstream components from clogging. Pore selection size must be carefully chosen; too fine and the filter becomes a significant restriction to flow, too large and residue particles can clog downstream components. This filter allows the user to quickly and easily change or clean the filter as needed.

11. Back Pressure Valve: Previous experience using spring-driven back pressure valves (alternatively known as pressure let-down devices) yielded poor pressure regulation. A slight buildup of 'sticky' particles easily clogged the system rendering backpressure regulation difficult. Additionally, pressure regulation of entrained liquid and gas mixtures under low flow is difficult for spring-operated regulators. Pressure letdown is an essential function of the CHTL system, by adjusting the pressure differential from inlet to outlet a stable flow rate can be achieved. Any disruption to the pressure regulation devices results in an immediate drop in system performance. An *Equilibar* spring-less diaphragm-operated valve (Model # EB1HP1) was identified and employed for this critical role. This model incorporates a flexible diaphragm in which one side is referenced to a high pressure source chamber, while the other to the inlet-outlet chamber. Whenever the inlet pressure (coming upstream from the CHTL system) is greater than the reference pressure the diaphragm moves up allowing the inlet stream to vent to the outlet port. This design accommodates low-flow and water-gas mixtures better than spring-driven regulators. The user simply dials in a set

reference pressure and the regulator will ensure that minimum pressure is held within the system.

12. Product Collection: Liquid and gaseous products exiting the back pressure valve, now relieved to atmospheric pressure, enter a simple 2.0 L beaker. Gaseous products are either sampled for composition or vented to an appropriate fume hood while liquid products are collected for further analysis.

4.2 Ohmic Heating: Background, Engineering and Prototype Iterations.

4.2.1 Introduction and Theory of Operation.

The principle of ohmic heating is fairly straight forward. An electric current is passed through a conductive media; the electrical resistance of that media causes a rise in its temperature. Collisions between traveling electrons and atomic ions within the conductor increase the martial ion's kinetic energy resulting in a temperature increase of that material. The following section will outline the underlying principles for employing ohmic heating of algal biomass slurries for a continuous HTL process.

According to *Joules 1st Law*, heating of a resistive media is proportional to the square of the current multiplied by the material's resistance. By incorporating Ohm's law, which is given by equation 6, one can deduce the general equivalent ohmic heating equations outlined by equation 7.

$$P \sim I^2 R$$

Equation 5. Joules 1st Law.

$$I = \frac{E}{R}$$

Equation 6. Ohm's Law.

$$P = I^2 R = IE = \frac{E^2}{R}$$

Equation 7. Equivalent forms describing ohmic heating in the direct current case.

Only two additional equations are necessary to describe the continuous ohmic heating process. The *Resistance* equations, which can be expressed in terms of slurry resistivity or conductivity, coupled with the media's *Heat Capacity* equation are all that is necessary to build the slurry heating models based on ohmic heating.

$$R = \frac{\rho L}{a} = \frac{L}{\theta a}$$

Equation 8. Resistance equation based on slurry resistivity or conductivity.

$$Q = C_{ps}\dot{m}\Delta\mathrm{T}$$

Equation 9. General heat capacity equation.

By condensing the *Equivalent Ohmic Heating* and *Resistance* equations into one model and setting that equal to the slurry *Heat Capacity* equation the resultant heating models in terms of slurry resistivity (Eq 10) or conductivity (Eq 11) can be readily derived.

$$\Delta\mathrm{T} = \frac{I^2\rho L}{aC_{ps}\dot{m}} = \frac{E^2 a}{\rho L C_{ps}\dot{m}} = \frac{EI}{C_{ps}\dot{m}}$$

Equation 10. Equivalent Ohmic heating models derived from slurry resistivity.

$$\Delta\mathrm{T} = \frac{I^2 L}{\theta a C_{ps}\dot{m}} = \frac{E^2 a\theta}{L C_{ps}\dot{m}} = \frac{EI}{C_{ps}\dot{m}}$$

Equation 11. Equivalent Ohmic heating models derived from slurry conductivity.

Where:

ΔT is temperature rise of the slurry measured in Kelvin (***K***)

E is potential difference across gap measured in Voltage ($V \sim \frac{\boldsymbol{kg*m^2}}{\boldsymbol{A*s^3}}$)

I is current flow measured in Amperes (***A***)

θ is conductivity of slurry measured in Siemens per meter $\left(\frac{S}{m} \sim \frac{\boldsymbol{s^3*A^2}}{\boldsymbol{kg*m^3}}\right)$

ρ is resistivity of slurry measured in ohm meters $\left(\Omega m \sim \frac{\boldsymbol{m^3 * kg}}{\boldsymbol{s^{3*}A^2}}\right)$
a is the cross sectional area of gap measured in square meters ($\boldsymbol{m^2}$)
L is length of gap measured in meters ($\boldsymbol{m}$)
C_{ps} is specific heat capacity of slurry ($\frac{J}{kg*K} \sim \frac{\boldsymbol{m^2}}{\boldsymbol{s^2 * K}}$)
$\dot{m}$ is mass flow rate of slurry ($\frac{\boldsymbol{kg}}{\boldsymbol{s}}$)
*Bold indicates SI base or derived units.

The heating models given in equations 10 and 11 outline the primary factors affecting the slurry temperature rise. Rapid heating can be accomplished by increasing the voltage potential or decreasing the slurry flow rate. Since the current passing through a substance is directly proportional to the voltage difference between the electrode points increasing the voltage potential dramatically increases the materials temperature per *Joules 1st Law*. A variable output power supply can be employed to regulate the voltage potential between the electrodes allowing the user to dial in the ideal voltage (and subsequent current) for the heating application. Varying the mass flow rate of the slurry can also be an effective way to manage the slurry temperature for ohmic heating processes operating from a fixed power supply. Increasing the material flow rate will result in smaller temperature rise because a greater mass of fluid will pass through the treatment zone diluting the amount of energy input into the fluid.

Temperature controllers can be incorporated to fully automate the heating process. A logically-controlled relayed output can be used to vary the ohmic heater's duty cycle. Assuming the slurry conductivity is compatible with the supplied voltage differential, a pulsed current could be supplied from a fixed power supply alleviating the need to incorporate an expensive Variac. This project chose to incorporate a Variac since the algal slurry's conductivity changes slightly from one batch to the next necessitating the ability to tune the voltage potential from time to time.

4.2.2 Engineering the Ohmic Heater.

The length and cross-sectional area of the slurry treatment zone play a critical role in the electric field uniformity as well as the voltage potential required to operate the heater. Shorter electrode gaps allow the user to employ lower voltage potentials to overcome the resistivity of the material being heated. Smaller cross-sectional areas also

increase the uniformity and concentration of the treatment zone by reducing current dead zones located away from the electrodes. For this project a relatively small power supply providing an operating output range 0-280 VAC was targeted to source current for the ohmic heater. Teflon heater mock-ups run under passive conditions (30-60 °C @ 0.101 MPa) using ionically adjusted tap water to reproduce measured algal slurry conductivities were employed to identify workable dimensions for prototyping a heater capable of operating under more extreme conditions. An internal electrode gap of 12.0 mm with a 6.0 mm diameter cross-section proved to effectively heat the tap media within the target voltage range. These treatment dimensions were subsequently used for producing the first generation ohmic heater prototype. Additional analysis, employing the heating model outlined in equation 11, yields a suitable range of ohmic heating treatment lengths of 9-50 mm when supplying additional target operation values.

Engineering the ohmic heater to run under continuous conditions in the sub and supercritical regions (200-400 °C @ 6-28 MPa) proved to be the most challenging task. Ohmic heating relies on utilizing a dielectric, or electrical insulating, material to provide a slurry treatment region in which the electric current is forced through the liquid. Since this project requires that material to withstand extreme conditions many traditional dielectric materials such as glass, rubber, Teflon and various other thermoplastics could not be employed. The unique properties of Macor, a machinable glass-ceramic with a fairly high tensile strength and working temperature limit, proved it to be an initial ideal candidate for the dielectric material. Table 5 outlines a few select properties of Macor which ideally suited it for our application.

Property	**Value**
Density	2.52 g cm^{-3}
Water Absorption	0.0%
Compressive Strength	345 MPa
Tensile Strength	90 MPa
Flexular Strength	94 MPa
Max Use Temperature	1000 °C
Dielectric Strength	40 kV mm^{-1}

Table 5. Select Macor Properties (Ferro Ceramic Grinding Inc).

Previous mock-up ohmic heating models using Teflon showed that a treatment column with dimensions of 12.0 mm long and diameter of 6.0 mm worked well at producing an acceptable temperature gain given the target voltage and slurry conductivity regions. These mock-ups only provide the internal treatment dimensions; they do not tell us the outside treatment region thickness needed for adequate safety. Since the dielectric region can be treated like a small piece of tubing with a known length (12.0 mm) and internal diameter (6.0 mm), we can estimate the outer diameter required to achieve a giving bursting pressure suitable for our application. Knowing the materials strength, Barlow's formula (equation 12) can be employed to calculate an OD necessary to provide an adequate safety margin.

$$BP = \frac{2S*T}{OD*SF}$$

Equation 12. Barlow's formula for calculating pipe bursting pressure.

Where:

BP is bursting pressure (psi)
S is material strength (psi)
T is wall thickness (in)
OD is outside diameter (in)
SF is safety factor

Selection of the proper OD for the Macor was calculated based on the ultimate tensile strength (90 MPa ~ 13,053 psi) provided in Table 5, along with estimates of required internal diameter (6.00 mm ~ 0.2363 in) for the treatment region. Theoretical bursting pressures were calculated for a range of OD's from 0.25-3.00 in based on a safety factor of 2. Figure 8 outlines a graphical depiction of the estimated working pressures of various OD's. Although the target pressure and the theoretical working pressure intersect at an OD of just 0.6 in, we chose to manufacture the first prototype with an OD of 2.0 in (50.8 mm). The increased safety margin, ease of machining and the immediate availability of larger 2 in OD Macor stock drove the decision to use that dimension for the initial prototype. The final dielectric strength of the machined Macor sleeve with and ID of 6.0 mm, OD of 50.8 mm and nominal width of 12.0 mm is estimated at 1912 kV from the center to outside and 480 kV across the width, more than enough to isolate our 0-280 VAC power source.

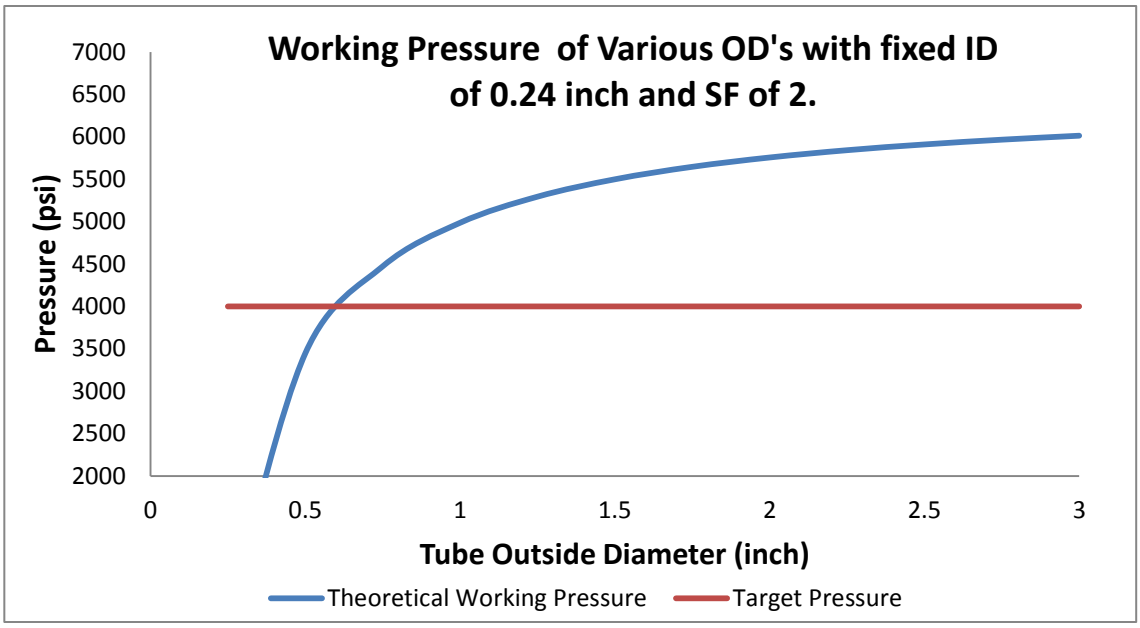

Figure 8. Theoretical working pressure of Macor tubing over a range of OD's using a fixed ID of 0.24 in and safety factor of 2. Working pressure calculated according the Barlow's formula.

Other components and dimensions of the ohmic heater were selected to provide compatibility to the existing CHTL system. Stainless steel tubing is used extensively throughout the system. Accordingly, 0.5 in OD SS tubing was incorporated into the ohmic heater to mate the inlet and outlet ports to the existing infrastructure. This tubing can also be utilized as the primary electrode source providing an adequate sealing surface can be achieved between the conductive electrode surface the dielectric isolation material. Giving the high temperature and pressure limits imposed by the CHTL system the identification and utilization of suitable sealing material also becomes an important consideration.

4.2.3 Prototype Iterations and Results.

4.2.3.1 1st Generation Prototype and Findings.

The first conceptual drawing of a proposed ohmic heater was devised in mid-October, 2011. Figure 9 outlines the basic schematic of the heating device. In this drawing the central positive electrode flange (blue) is insulated from the negative electrode flanges (green) by Macor sleeves (red). This design allows for two treatment

zones in which current can pass through to heat the slurry. Sealing of the device is achieved by tightening six bolts (orange) which span the length between the two negative electrode flanges. Malleable copper rings (brown) set between each flange and sleeve will provide a leak tight seal when compressed. Stainless steel tubing (yellow) of 0.5 in OD is welded to the negative electrode flanges providing plumbable sites to mate the heater to the existing CHTL system. With this general concept in mind, consultations with University engineers and machinists took place.

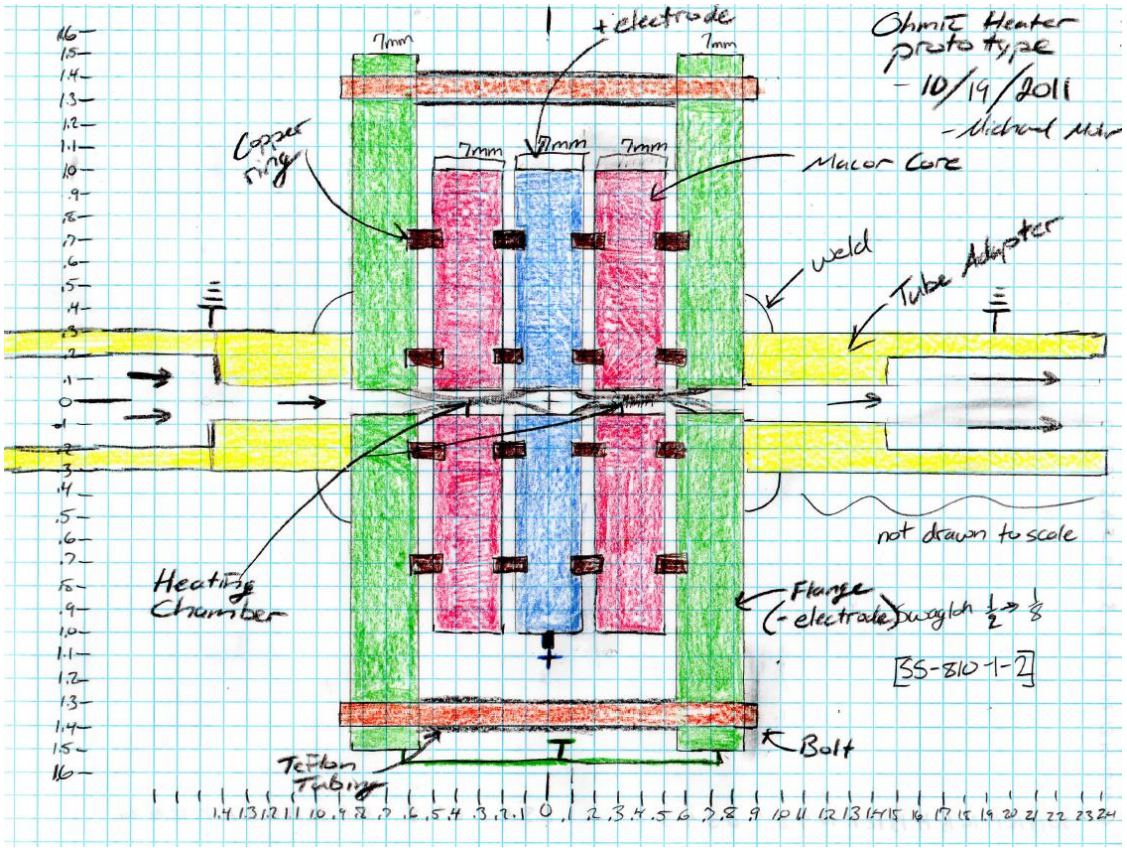

Figure 9. First conceptual drawing of the proposed prototype. Image produced by Michael Mohr.

Minor design revisions of the original concept were incorporated into the first generation device. Figure 10, provides a cross-sectional view of the final design and the fully assembled view of the heater. This design uses a small piece of SS tubing as the central positive electrode while SS tubing welded inside larger flanges are employed as the negative electrodes. Four thin copper gaskets are compressed between grooved edges

of the electrode and insulating Macor components and provide the high pressure seal. Like the conceptual design, bolts that span between the two negative Stainless Steel flanges provide the anchor points needed to compress the copper gaskets allowing the device to achieve an adequate seal. A threaded opening was provided in the outlet flange to allow for the incorporation of a thermocouple to measure the exit temperature of the heated media.

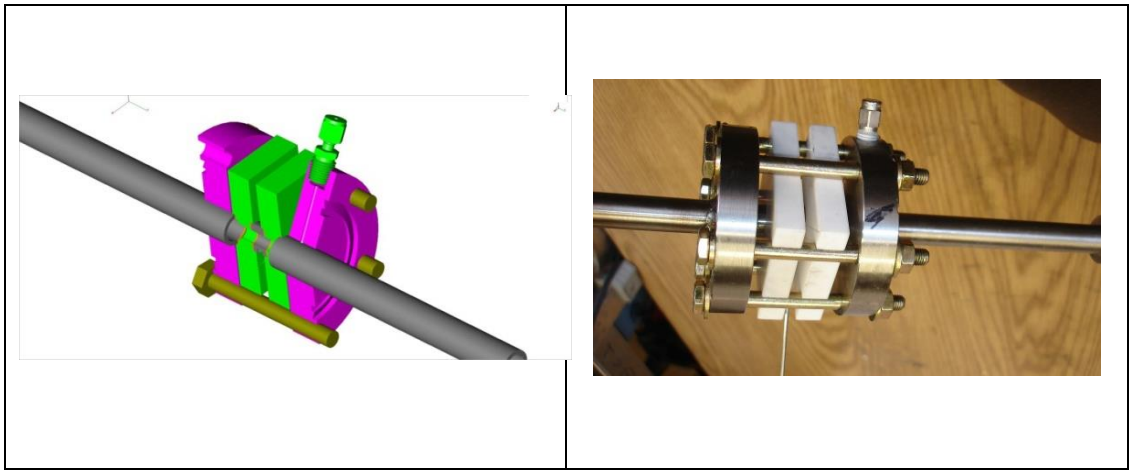

Figure 10. (LEFT) 3 dimensional drawing of 1st-generation ohmic heating prototype. Image provided by Dave Hultman Design. (RIGHT) Fully assembled heater as tested with CHTL system. Image provided by Michael Mohr.

The first prototype was delivered on January 19th, 2012 with lab trials carried out over the next three weeks. Pressure testing of the sealing mechanism was performed up to 6.89 MPa (1000 psi) using compressed air. To test for leaks, the device was charged with air and submerged under water for 30 minutes; no bubbles were seen indicating that the sealing mechanism was adequate. After plumbing the heater into the existing CHTL framework, pressure testing up to 17.2 MPa (2500 psi) was performed using liquid media, again no leaks were detected. Heating performance data was gathered from the device using ionically adjusted tap water (3.20 mS cm^{-1}) to emulate the electrical conductivity of the targeted algal paste feedstock. A *Milwaukee 2235-20* Clamp Meter and *Milwaukee 2217-20* Digital Multimeter were employed to monitor the electrical current and voltage supplied to the heater from the variable output transformer.

Trial testing of the heater yielded very promising results. A volumetric flow of 0.065 L min^{-1} of adjusted tap water with an initial temperature of ~50 °C could be heated

to 240 °C in ~0.01 min yielding an observed heating rate of 18,199.7 °C min^{-1}. This heating rate agrees well with the predicted heating rate of 16,499.3 °C min^{-1} given an operating voltage of 260 VAC and current draw of 3.0 Amps under the test conditions. Over ten hours of testing within subcritical conditions was completed before the sealing mechanism failed. Unfortunately, no tests were carried out using either algal or tomato paste to verify the heaters' ability to accommodate more viscous fluids.

Dissection of the heater revealed interesting observations. Although the SS316 tubing can be employed as an electrode material, rapid electrolytic passivation occurs which forms an insulating oxide coating in the inside of the tubing. As this mild dielectric layer accumulates it further impedes current flow, encouraging the electrons flowing within the treatment zone to travel farther in their pursuit of the path of least resistance. This phenomena lead to substantial lateral growth of a thick oxide layer which coated the internal wetted surface area of the tubing. As the electrons *searched* for the path of least resistance, a growing percentage of them traveled through the copper sealing gaskets back to ground. Unfortunately, copper appears to be more susceptible to electrolytic passivation and will degrade in much the same way as the neighboring SS components. As more electrons flowed through the copper gasket, electrolytic degradation culminated to point where the mechanical integrity of the gasket was lost and a blowout occurred. Additionally, microscopic stress fractures observed within the insulating Macor pieces suggested one of two things:

1. The dielectric pieces employed where too thin. Each piece measured 50.8 x 50.8 x 12.0 mm increasing the smallest width dimension would greatly enhance the strength of the Macor piece. However, since this increases the length of the treatment region, a larger voltage potential or increased slurry electrical conductivity will be required to overcome the increased resistance resulting from the widened treatment area.
2. Uneven loading of the heater by the six bolts could result in an uneven distribution of compression forces on the pieces. This non-uniformity greatly encourages micro-fractures as the components attempt to distribute uneven stress.

Given the promising performance of the 1st generation prototype, immediate development was started for the 2nd generation heater. Eliminating the degradation and passivation of the electrodes, re-engineering the sealing design and improving the compression mechanism where identified as the primary objectives for the next generation prototype. A host of fundamentally different heater designs, as seen in Figure 11, where explored which employed consumable electrode rods embedded within a dielectric core. The utilization of dielectric coatings such as alumina (for hard-anodized or micro-arc oxidation treated aluminum) as well as spray coated ceramics for stainless steel where explored. Given the relatively high cost and the unproven performance of these advanced technologies under subcritical conditions the decision was made to blend elements of the first generation heater with those of the newer concepts without the necessity of specialized coatings or surface treatments.

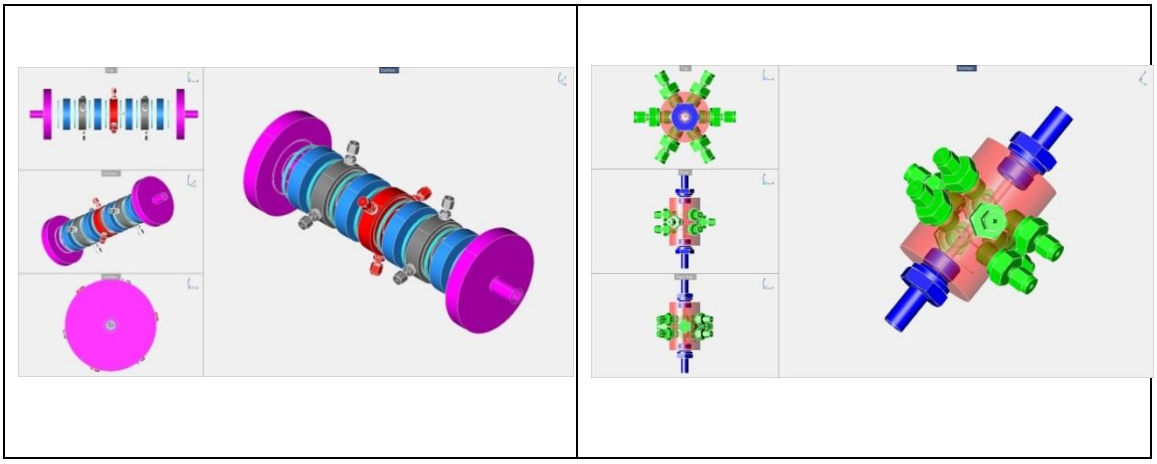

Figure 11. Ohmic heater concepts utilizing replaceable electrodes within flanges (LEFT) and within a dielectric solid core (RIGHT). Images provided by Michael Mohr

By incorporating a consumable electrode material such as tungsten, the deleterious effects of passivation were hoped to be mitigated. As the electrodes decay they can be periodically replaced depending on the heaters measured performance. The incorporation of 1/16 in tube adapters which house the electrodes also allows for flexibility in electrode selection. Various materials are readily available in 1/16 in stock OD's as welding rods from the TIG welding industry. The depth of each electrode can also be selectively gauged for each individual rod. Depending on electrode depth various electric and heating fields can be induced within the treatment region.

4.2.3.2 2nd Generation Prototype and Findings.

On June 4, 2012 the 2nd generation prototype heater was delivered to our lab for trial testing. Figure 12 provides a three dimensional rendering and fully assembled view of the device. This generation incorporated an additional set of Macor insulators which isolate the negative electrodes from the earth grounded circuit. Additionally, this generation incorporates redesigned Macor sleeves with the dimensions: 50.8 x 50.8 x 12.7 mm. Although, this generation shares a similar dimension, the geometry of the sealing mechanism should significantly improve the overall strength of each Macor sleeve, thus mitigating the previously observed stress fractures. In all, nine tube adapters are incorporated into the device to accommodate the replaceable electrodes. Each stainless steel flange holds 3 electrodes spaced 120 degrees apart allowing for a uniform treatment region. Additionally, a thin Macor sleeve is incorporated into the flange-treatment zone interface. This thin insulating piece will reduce the electrolytic potential of the SS flanges as the electrodes degrade over time. The geometry of this design spaces the center tips of each electrode at approximately 25.5 mm apart, which is significantly larger than the 1st generation's treatment gap of just 12.0 mm. The internal diameter of the 2nd generation heater is also slightly larger at 9.4 mm (0.36 in) compared to the 6.0 mm (0.24 in) internal diameter of the former. This dimension allows for a more seamless non-reducing internal diameter transition from the stainless tubing to the heating region.

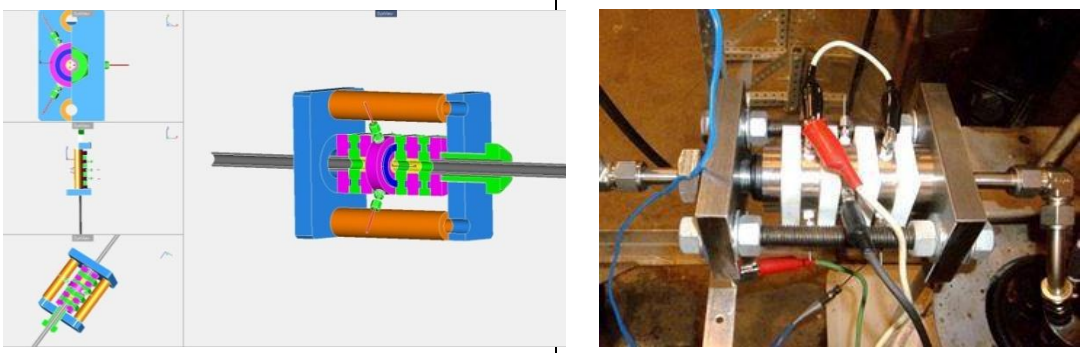

Figure 12. (LEFT) Three dimensional drawing of the 2nd-generation ohmic heating prototype. (RIGHT) Fully assembled heater plumbed into the CHTL system. Images provided by Michael Mohr.

High-pressure sealing of the device is achieved by compressing Grafoil, metal reinforced sheets of graphite, gaskets into a recessed opening within the Macor sleeves. These gaskets are chemically inert and are developed for continuous use in temperatures up to 450 °C. The gaskets are held in place by an overlapping lip machined into each stainless flange. This lipped seal reduces the chance of gasket blowout while also reducing the overall footprint of the device. Initially, the sealing faces of the Macor and SS flanges within the grooves and lips were smooth. Trial testing of this design yielded weeping leaks of water at high pressure. Ideally, the Grafoil should be compressed into small grooves to achieve a leak-tight seal at pressure. After re-machining the sealing faces to incorporate a dual 0.5 mm recessed groove in which the Grafoil could seat itself, a high-pressure seal was achieved.

The necessary strength required to compress the gaskets against each sealing face of the Macor sleeves and SS flanges is obtained by tightening a singular central bolt anchored on a plate. This plate is then connected to a second plate via two anchoring bolts. The incorporation of a self-aligning spherical washer (not pictured in figure 12) on the central tightening mechanism ensures a uniform compression force is loaded onto the assembly. This washer allows for an alignment correction of 1-2° between the plates while significantly simplifying the tightening procedure and reducing non-uniform loading stress on the heater's brittle components.

On July 5th 2012, initial trials were carried out with 2nd generation heater with grooved sealing lips. It was found that producing a leak-tight seal under moderate pressure was a challenge; therefore heating tests were carried out at ~2 MPa (~300 psi). A flowrate of 82 ml/min with a slurry conductivity of 4.32 mS cm^{-1} was employed. Nominal heating was achieved by supplying 276 VAC @ 0.82 Amps to the heater. When an attempt was made to increase the torque on the central compression mechanism one of the four insulating Macor sleeves fractured. It was determined the uneven compression forces, even with the spherical washer employed, resulted in stress fracturing the ceramic Macor material. Given Macor's inherent susceptibility to stress fracturing, the decision was made to identify and incorporate a substitute dielectric gasketing solution.

A new gasket material was identified a few days later. Mica was found to be an ideal candidate for our application. Mica gaskets are essentially flecks of Mica rock

embedded within a resin core. Multiple layers of this Mica laminate are stacked together and used to make a typical gasket sheet. Giving its unique manufacturing process Mica gaskets can be made in nearly any thickness depending on the amount of layers the application requires. These gaskets find wide use in the petro-chemical industries as well as in areas where electrical isolation is critical. Mica gaskets display dielectric strengths in excess of 25 kV mm^{-1} and are rated for continuous use temperatures applications exceeding 1000 °C (Mica Gasket Material). Modifications were made to the 2nd prototype heater to accommodate 1.5 mm thick Mica gaskets. As seen in figure 13, small overlapping grooves where incorporated into the stainless steel electrode housing flanges to improve the sealing performance. One major benefit of this modification was an overall reduction in the electrode-to-electrode treatment volume. With the new Mica gaskets installed the electrode-to-electrode treatment length was substantially reduced from 25.5 mm to just 13.5 mm. As expected, this resulted in improved heating performance at reduced voltage potentials for our targeted slurry.

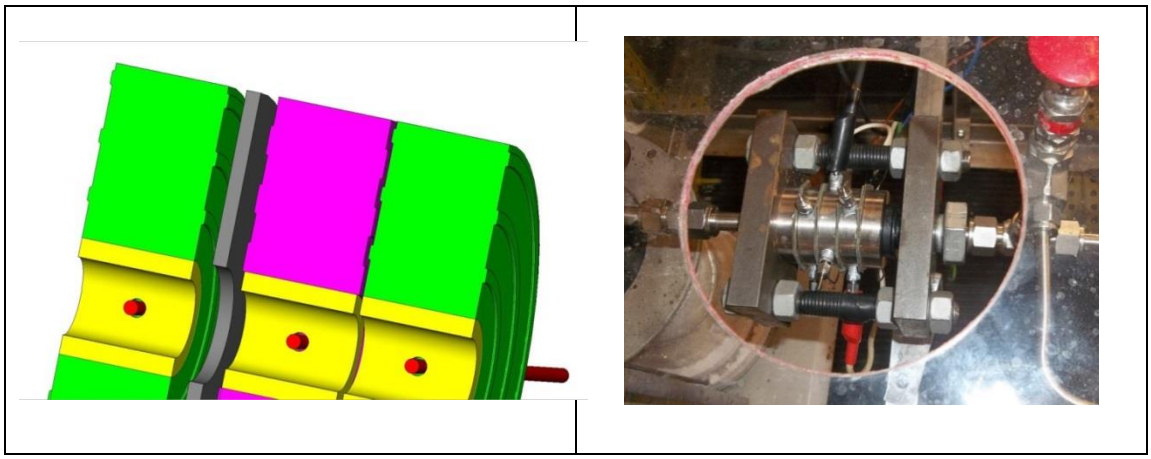

Figure 13. (LEFT) Three dimensional drawing of 2nd-generation ohmic heating prototype with Mica gasket seal. (RIGHT) Fully assembled heater plumbed into the CHTL system. Notice the shorter overall footprint. Images provided by Michael Mohr.

As mentioned earlier, one of the main advantages of the 2nd generation heater was the capability to test a variety of different electrode materials. Qualitative data was gathered for Copper, Tungsten, 316SS and Graphite electrodes. The results of those tests are located below. A single high pressure test at 27.6 MPa (4,000 psi) was performed on the CHTL system with this modified heater installed. No apparent leaks or material

failures were detected on the heater for the duration of the test, although the other parts of the CHTL system, particularly, the gravity clarifier needed adjustment to sustain this working pressure.

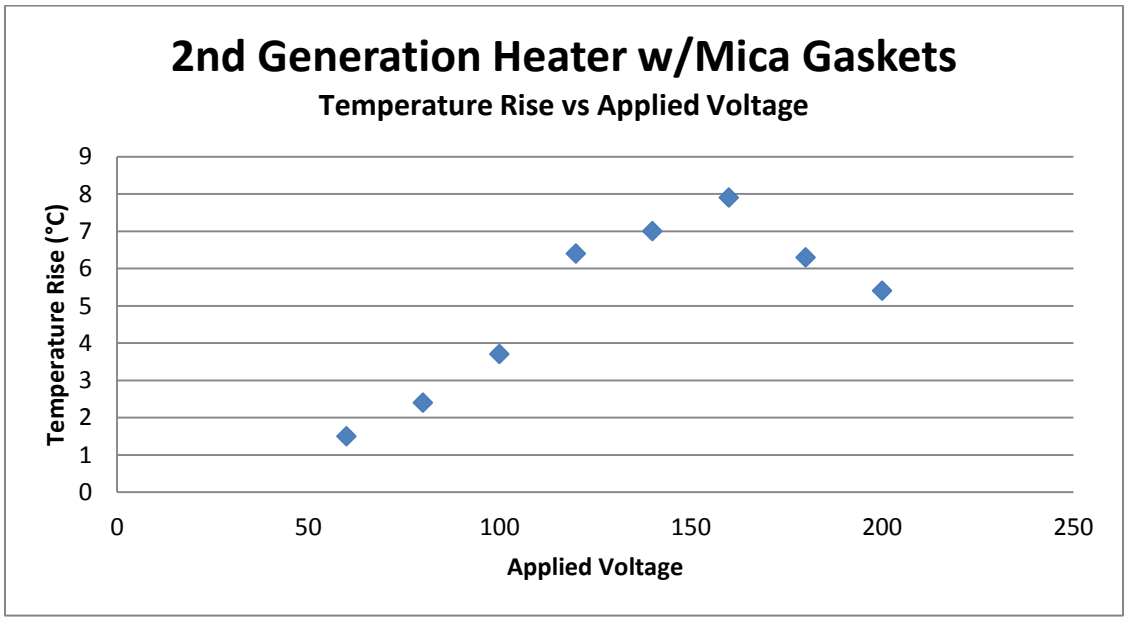

Figure 14. 2nd generation heater performance curve under 1,500 psi, 106 ml min-1, and slurry conductivity of 5.557 mS cm-1.

After a few trial tests were conducted it was found that the 2nd prototype heater suffered from some of the same pitfalls as the 1st generation. It was noticed that the first 3-4 minutes of each trial test, of which fresh electrodes were used, the performance of the heater followed a typical exponential temperature rise. However, after some time the heater's performance would unexpectedly drop off. This phenomenon can be readily seen in figure 14. The first few minutes of heating, while ramping the voltage from 0 to 160 VAC, the temperatures rise was fairly predictable and followed a well-defined path. After the heater was operational for a few minutes, the heating performance would drop off over time. Real-time current measurements indicated that even as the voltage was increased to the heater its total amperage draw in many cases would diminish. This is contradicted by what is predicted by Ohm's Law which states that in a given circuit with a fixed resistance a rise is applied voltage will result in a corresponding rise in the current drawn through it. To compound this observation, electrical current measurements with fresh electrodes employing higher applied voltages conducted within the first few minutes of an experiment resulted in the current to voltage relationships predicted by

Ohm's Law. Performance data suggested that the resistivity of the circuit would increase over time independent of the initial applied voltage.

Dissection of the various electrode tips used showed significant tip passivation and fouling. This phenomenon was noticed in the first generation as well. As each fresh electrode would begin to decay its ability of transmit electrons to the slurry would diminish. Consequently, the electrode's performance over a very short period of time resulted in reduced current flow even if the applied voltage potential between them was increased. Nearly all of the electrodes tested exhibited similar decay characteristics. Figure 15 shows the four primary electrodes tested after employment within the heater. Tungsten electrodes exhibited extensive mass lose and minimal deposition of impurities on the exposed electrode surface area. T316SS and Copper electrodes both rapidly formed a highly insulating dielectric oxidized coating after minimal exposure. Even though electrode replacement is fairly easy these materials were ruled out for further testing because of their relatively short life expectancy. Extensive testing proved Graphite to be the most robust material, although brittle in nature, it displayed no passivation and minimal mass lose as the experiments were carried out. Graphite's unique qualifications for ohmic heating applications have been explored earlier in our lab; however, no attempts were previously made to employ it under high temperature and high pressure scenarios.

Figure 15. Electrode materials tested in the 2nd generation heater. Clockwise from top left: Tungsten, T316SS, Copper and Graphite. Images provided by Michael Mohr.

Once Graphite was identified as the ideal electrode material, the heating model developed in section 4.2.1 was used to help evaluate the ohmic heater's performance. Equation 11 was employed in an interactive spreadsheet so raw performance data could plotted against the predicted temperature rise based on the process flowrate, slurry conductivity and the heater's physical dimensions. Good agreement between the model and the raw data, as seen in figure 16, indicate the heater is performing as predicted. Additionally, linear relationships between either the current squared and voltage squared plotted against the slurry's temperature rise further suggest the heater is performing as predicted by Equation 11.

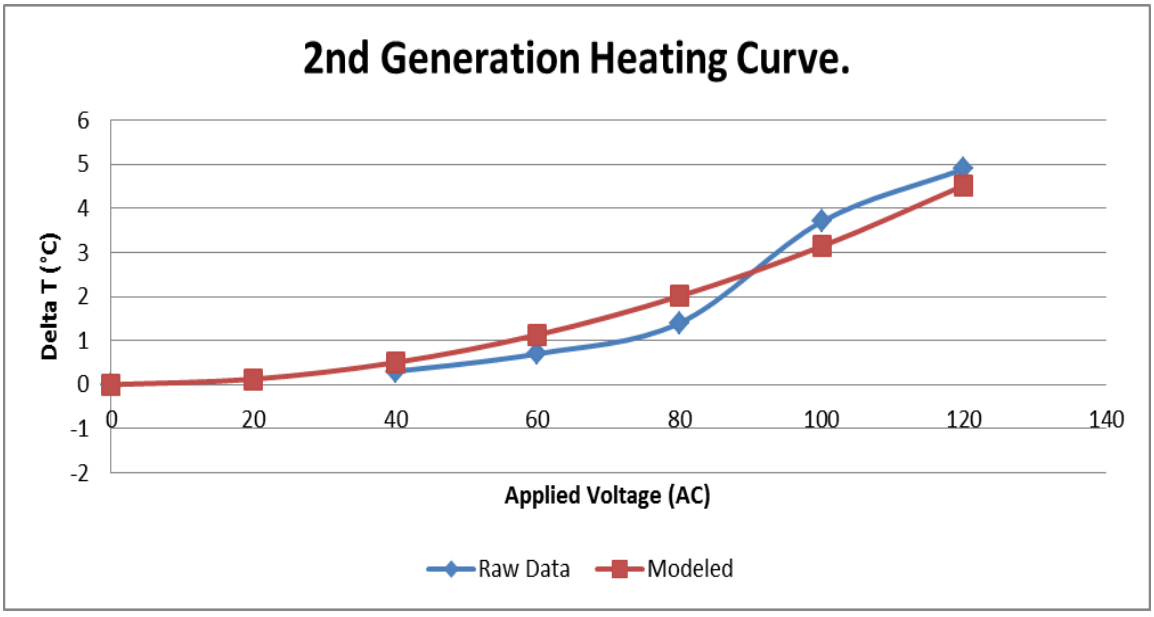

Figure 16. 2nd generation heater raw data vs modeled performance. Slurry conductivity: 4.9 mS cm-1, flowrate: 190 ml min-1, pressure: <100 psi.

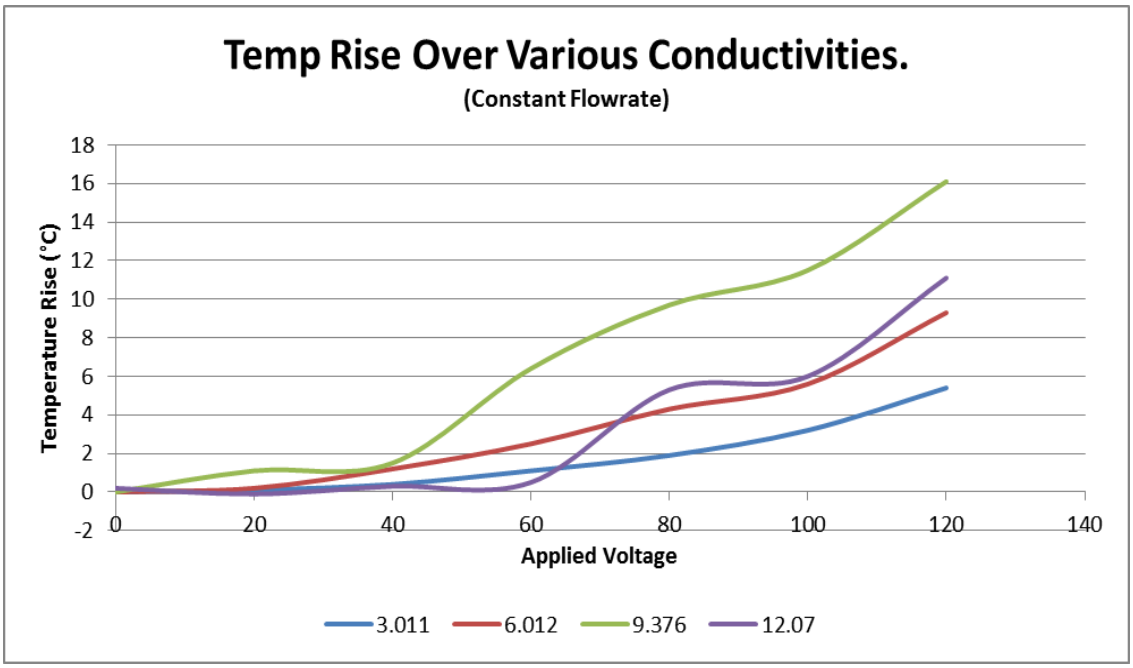

Figure 17. Temperature rise of various slurry conductivities under a constant flowrate (190ml min^{-1}) and defined voltage potential.

The effect of various slurry conductivities was assessed with the ohmic heater using graphite electrodes. In applications where the slurry conductivity is very low, high applied voltages will be necessary to overcome the high resistivity of the slurry and resultant resistance of the treatment path. Conversely, in applications where the conductivity is too high, reduced heating performance can be expected as the slurry begins to act more like an ideal conductor. Much like a copper wire with very low resistivity, the electrons are transmitted to very high currents, without substantial heating.

Prior tests using tap water ionically adjusted with NaCl to reflect in-situ algal slurry conductivity measurements have already proven that ohmic heating can work for this conductivity range. However, a series of experiments were conducted which aimed to test our heater's capability to heat various slurry conductivities under a defined voltage range. Adjusted slurry conductivities of 3, 6, 9, and 12 mS cm^{-1} where tested under similar conditions to elucidate the effects of the slurry conductivity in our ohmic heating process. Results from this experiment shown in figure 17 reveal that all conductivities tested within the voltage potential of 0-120 VAC effectively heated the slurry. As expected, lower slurry conductivities resulted in less heating, while increased conductivities resulted in higher heat gains to a point. Very high conductivities resulted in

decreased heat gain as the slurry began to act more like an ideal conductor. Results from this experiment suggest slurry conductivies in the range of 3.0-9.0 mS cm^{-1} would be ideal for our application. Lab measurements of algal slurry conductivities ranged from 4.16-4.25 mS cm^{-1}.

The effect of slurry flowrate was also explored. Higher process flowrates should require more energy to produce the same temperature rise. Data gathered under various flowrates with the same slurry conductivity support this observation. Low process flowrates had a longer residence time within the ohmic heater's treatment region, thus resulting in increased thermal gain. Conversely, higher process flowrates, as witnessed in

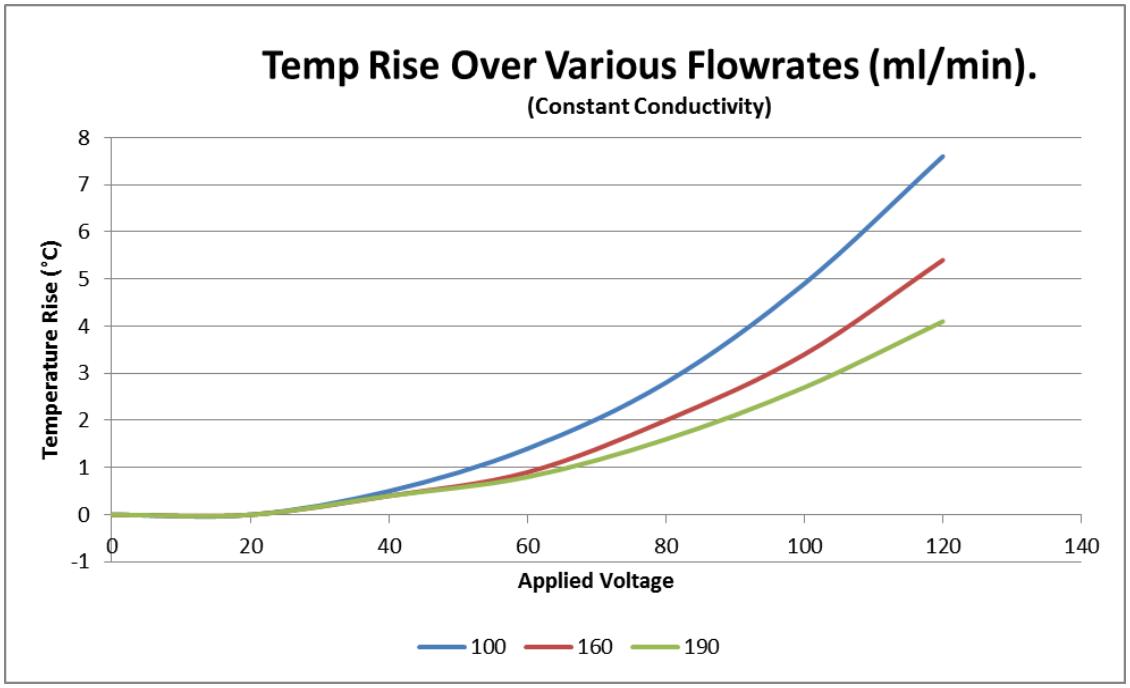

Figure 18. Temperature rise of the slurry under various process flowrates with same conductivity over a defined voltage range.

figure 18, resulted decrease thermal gain. Ohmic heating processes requiring higher thermal gain would need to employ higher applied voltages or higher slurry conductivities to increase the electric current consumed in the process.

Process data gathered from the modified version of the 2nd generation prototype allowed us to achieve a few milestones within this project. First, Mica gaskets were found to be an ideal insulating material for our process. Second, Graphite was identified as the best electrode material for sustained heating applications. Third, the heating model

derived in section 4.2.1 can reliably predict the expected temperature rise based on the process conditions and the heaters physical geometry. Finally, the anticipated effects of slurry conductivity, and flowrate where verified with real world data. However, the success of this design iteration did have a few shortcomings.

The relatively short treatment area resulting from the thin Mica gasket resulted in a high potential of flange-to-flange arching under higher voltage potentials. This phenomenon was noticed independent of electrode material. Sever arching could easily result in catastrophic failure if the arch path were to occur in an unfortunate area. The failure would be compounded if it occurred while the system was under sub-critical conditions. Thus, a small centrifugal pump was employed to carry out testing under very low pressure scenarios. Because this pump could only produce ~10 psi of forward pressure, the operating temperature of the heater was limited to <100 °C so steam production would be avoided. The use of an existing high pressure piston pump was ruled out because it lacked adequate flow control and posed a safety risk if a leak occurred downstream in the system. Work on the 3rd iteration of the ohmic heater began in earnest to address the remaining issues and improve the critical design characteristics of the 2nd generation's findings.

4.2.3.3 3rd Generation Prototype and Findings.

The qualitative data gathered from the 2nd generation heater was used to guide the development of the final iteration. To help eliminate the arching risk posed by the geometry of the adjacent electrode housing flanges it was proposed to machine a tapered void on each flange. The gap created by the taper could be filled with an insulating sleeve to permanently eliminate the arching potential in the future. The taper was designed so the shortest arch path, should it occur, would always travel from electrode to electrode, never from flange to flange.

Additionally, the electrode housing was modified to take advantage of Graphite's unique qualifications. The primary 1/16 in OD electrode materials were eliminated and replaced with a 9.40 mm ID x 15.0 mm OD x 8.80 mm thick Graphite sleeve. A small spring is used to transmit current to the electrode while also providing an anchor point for the sleeve. The stainless steel housing was scaled up to accommodate the new tapered

design and was machined to seal against the Mica gaskets. The final electrode-to-electrode gap when assembled is 15.3 mm; the next shortest potential arch path is ~23.0 mm from electrode-to-flange or ~29.0 mm from flange-to-flange. Assuming the Mica gasket holds its integrity, this design nearly eliminates any arching potential.

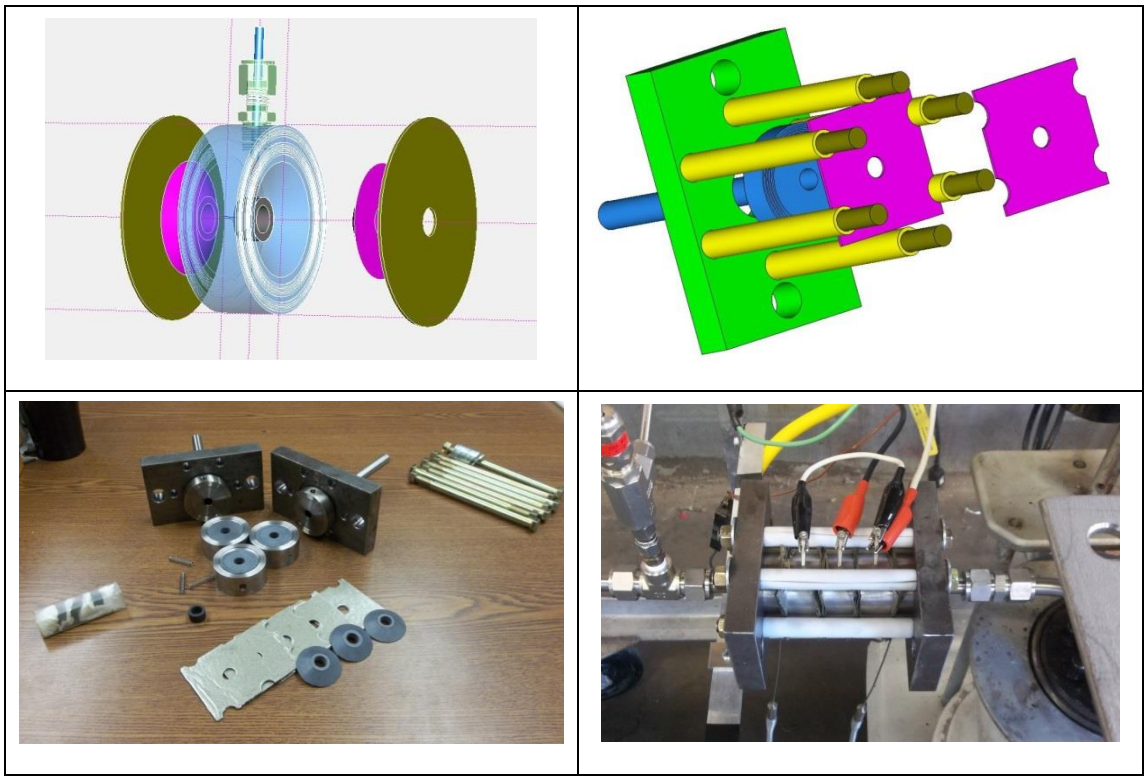

Figure 19. Clockwise from top left. (1) Flange, insulator and Mica gasket. (2) Compression assembly. (3) As-built and installed into CHTL Framework. (4) As delivered before assembly. Images provided by Michael Mohr (1, 3 & 4) and Dave Hultman Design (2).

The clamping mechanism developed is a hybrid between the previous generations. Two anchoring plates, along with six Teflon insulated tie rods were used to compress the SS flanges and Mica gasket assembly. With this design the spherical washer was removed and uniform clamping was achieved by following the standard torque sequence for a 6 bolt pipe flange. Periodic re-torqueing was necessary as the Mica gaskets seated into the flange sealing faces.

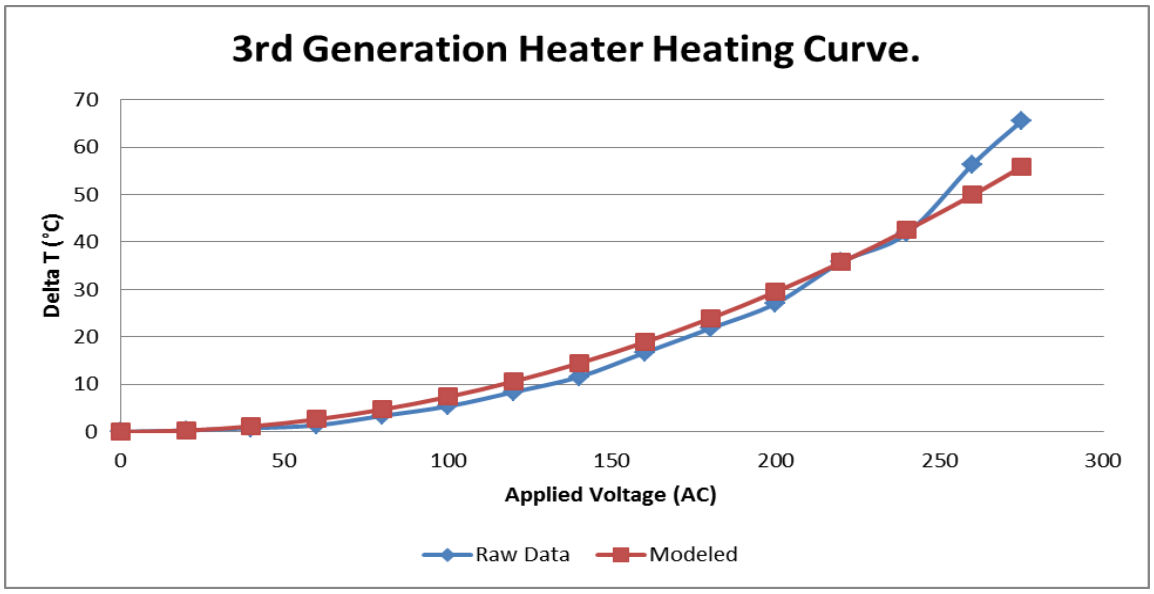

Figure 20. 3rd generation heater raw data vs modeled performance. Slurry conductivity: 6.84 mS cm-1, flowrate: 120 ml min-1, pressure: < 100 psi.

Preliminary data gathered from the 3rd generation heater installed in the existing CHTL framework was very promising. Again a small centrifugal pump was used to generate a consistent flowrate under low pressure. Results from an experiment, summarized in figure 20, with an adjusted slurry conductivity of 6.84 mS cm^{-1} produced very good agreement with the model's predictions. A correlation factor of 0.9923 can be observed between the raw and modeled data temperate rises. Again linear relationships, as shown in figure 21, are readily apparent between the voltage squared and amperage squared to the temperature rise.

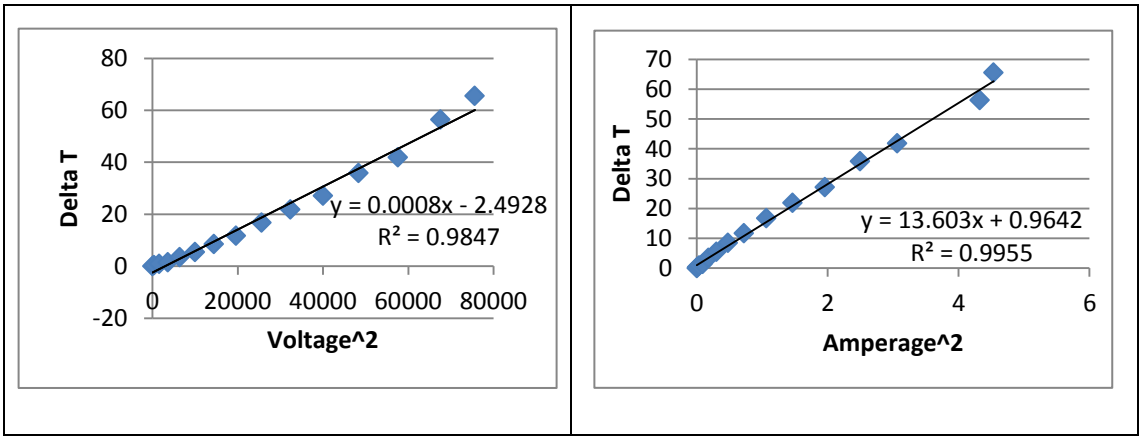

Figure 21. Linear associations between Voltage^2 and Amperage^2 related to temperature rise as predicted by Eq 11. Same experimental conditions as figure 20.

With performance data gathered under low pressure conditions the final trial necessary to meet the CHTL's design parameters was elevated pressure. To perform a controlled high-temperature and high pressure experiment a new pump was ordered. An Altech Model 301 HPLC pump was ordered from Grace Scientific. This pump is designed to deliver an accurate flowrate from 0-10 ml min^{-1} at pressures up to 42.0 MPa (6000 psi). Additional safety modifications were incorporated within the lab area to ensure worker safely. An aluminum reinforced ballistics glass barrier was constructed to protect the operator against system blowout. As a triple redundancy against steam, projectile and electrical hazards an 8' x 6' sheet of shatter resistant Plexi-glass was installed between the control station and the reaction area.

New power and thermocouple transmission lines were installed to provide extra distance from the reaction system. Wiring to and from the Variac, as well as, current and voltage testing leads were relocated to facilitate increased user safety. Personal protection wear, including high voltage gloves and face-masks were also purchased.

A test at sustained high pressures of 22.1 MPa (3200 psi) was carried out for a period of 2 hours to check for system leaks. Periodically, the flowrate coming out of the system was checked to ensure no leaks occurred while the system was under pressure. Output flowrates matched closely with the displayed flowrate of the HPLC pump. Discrepancies, though small, were likely attributable to residual air in the system that could not be purged while the system was initially charged. After no leakage was verified an experiment was conducted to see if the heater could attain super-critical conditions of 22.1 MPa (3200 psi) and 374 °C.

Conducting an ohmic heating experiment under extremely low flow conditions can be problematic. The potential for run-a-way heating is very likely. The electrical conductivity of saltwater increases as its temperature rises. If the residence time of the slurry inside the heating apparatus is long, a large amount of heat can be transferred to the housing which can then preheat the incoming fluid, thus resulting in net decrease in overall resistance. This phenomenon is minimized under high flow conditions where minimal preheating can occur. Results from figure 22 suggest this happened during the high temperature test. The raw data temperature rise trailed the modeled prediction until the supplied voltage was held constant at 160 VAC for a period of 20 minutes. During

this time, heat was transferred from the slurry to heater's mass. Gradual run-a-way heating was noticed at the constant voltage level of 160 VAC. During the time the experiment was held at this level the supplied current ramped from 3.2 to 4.6 amps fairly quickly. As the heater's temperature stabilized, less preheating was noticed. Unfortunately, a supply fuse blew during the test at a constant supply of 160 VAC. Once replaced, the Variac was set to supply 180 VAC to the heater, again, the same pre-heating phenomena was noticed.

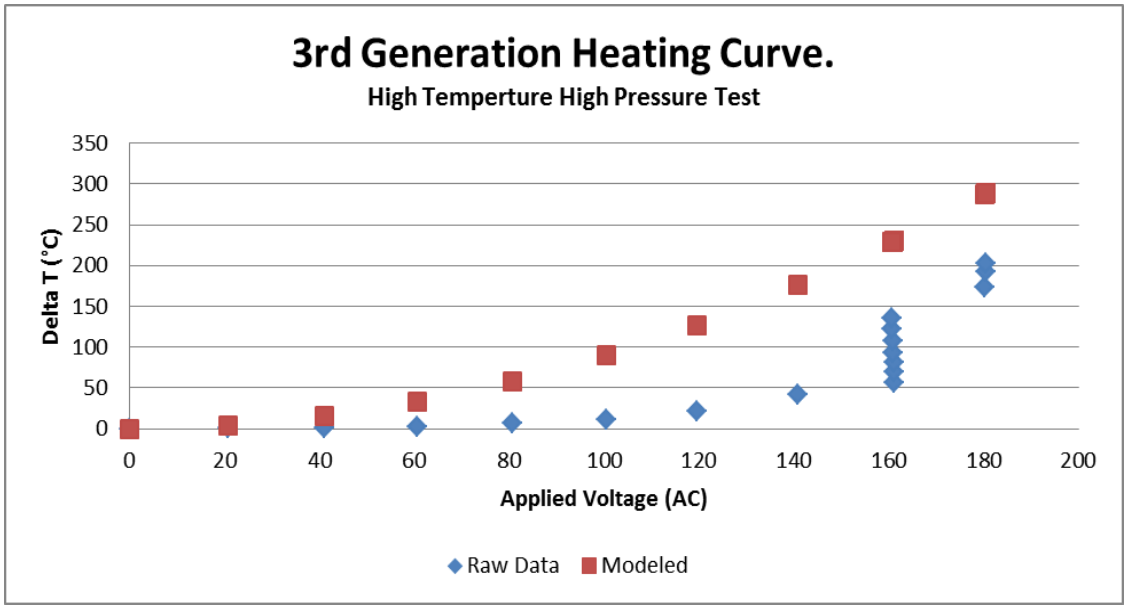

Figure 22. 3rd generation heater raw data vs modeled performance. Slurry conductivity: 6.85 mS cm-1, flowrate: 10 ml min-1, pressure: 3200 psi.

The heating model appears to be predicting quite well the final equilibrium temperature of the ohmic heating process. An electrical fault from the breaker supplying the lab receptacles limited our ability to fully reach super-critical conditions. However, a final output temperature of ~220 °C was readily attained indicated that the heating apparatus is functioning as expected. While waiting for the system to cool down, one of the Mica insulating gaskets let loose. Fortuitously, this happened while not supplying voltage to the heater. Examination of the Mica gasket revealed accelerated mechanical degradation from wetting. The Mica gasket material employed is recommended for dry applications, wetting appears to significantly degrade its mechanical strength.

Visual inspections of the heater's Graphite electrodes, insulating sleeves and flange housings appear to look good. Minimal mass lose was noticed on the Graphite

electrodes. The Graphite edges in direct contact with the slurry treatment area appear to be slightly chamfered compared to the edges away from the contact area. Additionally, caliper measurements reveal a slight enlargement of the central electrode's ID measurement by ~0.05 mm. No passivation or material deposition was noticed on the electrode faces. The insulating sleeves have also withstood the high temperature and pressure well. Again, no apparent degradation was noticed on their surfaces.

Research trials utilizing the heater within the existing CHTL framework support further work to improve its reliability and safely. We are reaching out to Mica gasket manufactures to identify a suitable substitute for the current Mica gasket. Several different resins can used to produce the Mica gasket sheets. Identifying one suitable for wet applications is our next priority. It is also proposed that further increasing the sealing surface area of the flanges would reduce the wetting area of the current Mica gasket; however, this modification would also require higher compression forces to overcome the enlarged area. Both options are currently, being considered.

4.3 Pressure Regulation.

4.3.1 Inlet and Outlet Regulation.

Regulation of the CHTL system's inlet and outlet pressures are imperative. A controlled flow is achieved from front to back by regulating the pressure drop from front to back. A large pressure drop will result in increased flows, while a small drop with result in decreased flows. Inlet regulation was initially controlled by a Graco high pressure fluid regulator Model #: 238894, this regulator is designed to convert a high pressure source of up to 41.4 MPa to a controlled output range of 3.44-27.6 MPa using low pressure process air.

Pressure letdown was achieved with an Equilibar backpressure regulator Model #: EB1HP1. This regulator employs a flexible diaphragm in place of a tradition spring and needle setup. By referencing a high pressure source such a gas cylinder this regulator is able to accommodate gas and fluid mixtures under extremely low flow conditions. Coupled to a high-pressure air cylinder with a venting regulator, precision backpressure regulation can be achieved.

Incorporation of the Graco regulator was useful to reduce and regulator the output of the high pressure Graco Merkur Piston Pump (Model # 040.035). As testing for the 3rd generation heater began the necessity of this regulator was diminished. Since the Altech HPLC pump was capable of producing a stable high pressure outlet on its own, only the Equilibar back pressure regulator was needed. The flowrate of the system can be dialed in on the HPLC pump, while the backpressure can be set via the reference gas connected to the backpressure regulator. Reproducible flowrates and stable pressures can be readily set within the CHTL system utilizing this combination. Given the flexibility and reliability of this method of flow and pressure regulation, detailed experiments can be designed to modify the exact residence time of treatment under the required reaction temperature for future CHTL experiments.

4.4 Hybrid Reaction Chamber.

4.4.1 Description of Modifications.

Previous attempts using a modified Parr Reactor Model #: 4575 within the existing CHTL framework proved fruitless. Given the larger thermal mass of the reaction vessel and relatively small supplied heater, the contents of the reaction vessel would take nearly 3 hours to reach a typical set point temperature of ~320 °C resulting in an effective heating rate of ~1.66 °C min^{-1}. As stated earlier, much of this time is a direct result from the thick stainless walls of the reactor restricting heat flow from the external band heater to the internal fluid. Another pitfall of this reactor is the limitation of including a heterogeneous catalyst. Because fluid must flow through small ports granular catalysts could not be used. Previous research employing a plug-flow type reactor also proved difficult. Significant fouling and blockage was apparent when laminar flow conditions were present. Although no previous experiments were completed using heterogeneous catalysts, restricted flow issued caused by char accumulation were anticipated.

Given Ohmic heating's ability to rapidly and uniformly heat the target slurry, it was proposed to plumb the heater directly to the inlet port of the existing Parr Reactor. In this setup the ohmic heater is essentially and instantaneous preheater for the reactor. Consequently, the heating load required by the Parr Reactor is greatly reduced. Since the fluid entering the reactor is at or near the desired reaction temperature, the Parr Reactor's

external band heater has adequate capacity to maintain the reaction temperature. Increased system throughputs can now readily be achieved without waiting for the Parr Reactor to reach reaction temperatures. Since the ohmic heating process also alleviates some of the known issues with more traditional contact heating methods, less charring and potential fouling issues are also present.

The ability to incorporate non-homogenous catalysts within the reactor was desired. Although many heterogeneous catalysts have been successfully employed in previous HTL research, few have been employed in continuous flow through experiments. Plug flow reactors are more suitable for housing solid catalysts; however they tend to clog almost instantaneously even when minimal char formation is present. Thus, it was proposed to modify the current Parr Reaction vessel to accommodate solid granular catalysts while minimizing the clogging potential.

Since the Parr vessel is already outfitted with a stirring mechanism and it contains a relatively large reaction volume a screening device was designed, figure 23, to install on the outlet port of the reactor. Two screen holders, each with a wetted filtering surface area of 1.5 in^2, are clamped to a central frame which is plumbed to the reactor outlet. The screen pore size can be easily changed according to the catalyst's granular size by removing four machine screws. A maximum of two screen holders can be installed inside the Parr reactor giving a nominal filtering surface area of 6.0 in^2. This arrangement now allows for the incorporation of heterogeneous catalysts and reduces the detrimental effects of charring and tarring within the reaction vessel which would otherwise plug other catalyst beds.

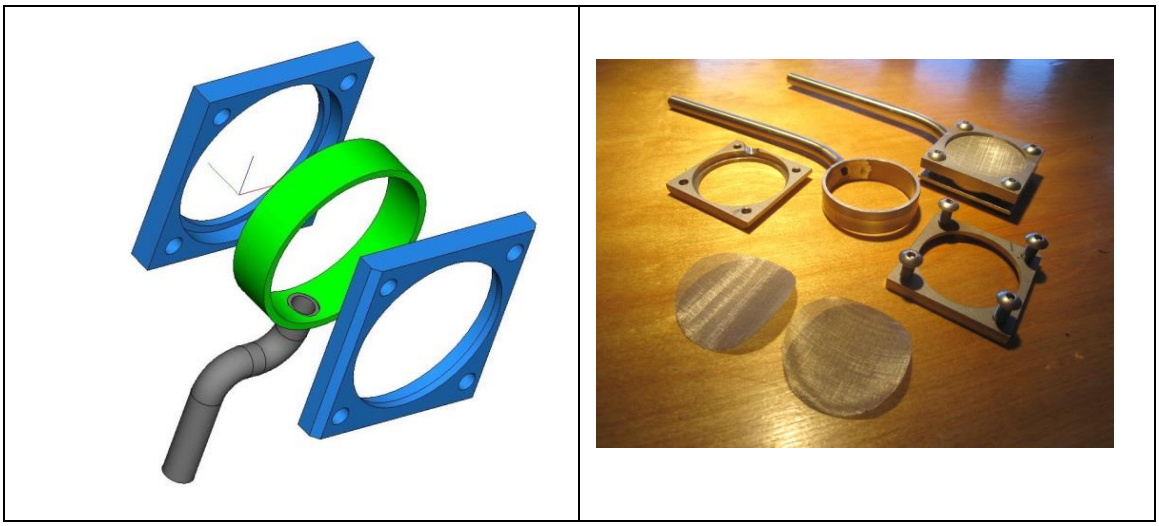

Figure 23. (LEFT) Prototype render of the outlet filtration screen holder for Parr Reactor. (RIGHT) Filtration screen assembly as delivered from machinist. Images provided by Dave Hultman Design.

CONCLUSIONS

Over the course of developing a fully functional continuous hydrothermal liquefaction system a variety of challenges needed to be addressed. An extensive literature review of various biomass processing techniques revealed synergistic opportunities between existing hydrothermal liquefaction technologies and slurried biomass sources such as algal pastes. An attempt was made to construct a heavily modified system to accommodate a host of slurries such as algal pastes. Within our attempts to improve the overall efficacy of the process we developed a novel high temperature and high pressure heating technology ideally suited for HTL processing. Additionally, we modified an existing reaction vessel to accommodate various catalysts one might use in HTL experiments.

The ohmic heating technology developed underwent a host of design iterations. In all, four distinct prototypes were tested. Depending on process conditions exceptional heating rates in excess of 16,000 °C min^{-1} and temperatures differential of ~200 °C with operating pressures of 3,200 psi where achieved. A heating model incorporating the targeted slurry's electrical conductivity, process flowrate, and the physical dimensions of heater's treatment area was derived and used to evaluate the heater's overall performance. The effect of slurry electrical conductivity and process flowrate was also

explored. As anticipated, a defined conductivity range of 3.0-9.0 mS cm^{-1} proved to be ideal for our targeted processing voltage.

Ceramic Macor and a Mica gasket sheets were evaluated for their effectiveness as the primary dielectric component of the heater. Although, earlier iterations of the ohmic heater utilized Macor effectively, its intrinsic brittle nature precluded it from further trials which required increased compressive forces. Mica gaskets proved to work quite well under both high temperature and high pressure scenarios. Although recommended for dry applications we successfully utilized it to achieve sub-critical (~220 °C @ 3,000 psi) HTL processing conditions.

Overall improvements were made to the flow and pressure regulation components for the CHTL system. It was found that a high pressure inlet regulator coupled with the cylinder referenced diaphragm regulator provided a smooth pressure gradient when utilizing the high pressure Graco Merkur piston pump. Conversely, only the backpressure regulator was required if using the smaller Altech HPLC pump to achieve steady flow and pressure gradients.

By coupling the ohmic heating device directly to Parr reactor inlet it was observed that higher system throughputs could be achieved without sacrificing the target reaction temperature inside the Parr vessel. By ohmicly preheating the biomass slurry better quality control can be achieved. Additionally, a screened outlet device was developed to filter the outlet of the reactor. This filter allows the user to include heterogeneous catalysts directly inside the reaction chamber without necessitating the use of a plug-flow type reactor. This capability significantly reduces the complications arising when char formations form inside the reactor.

RECOMMENDATIONS

With the developed system in place a researcher can now successfully study the effects of residence time, pressure, temperature, catalysts and process gases in a continuous system under near super-critical conditions. This work has resulted in a significant breakthrough and utilization for ohmic heating technologies. To our knowledge, we are the only research group attempting to reap the benefits of ohmic heating under HTL conditions. Our developments have been a direct result of many trial

and error experiments, calculated risks and some luck; however, improvements to the overall ohmic heating apparatus can be made. Identifying and integrating other suitable dielectric materials has been acknowledged as a top priority. Although Mica can be employed, it susceptibility to water limits its long-term viability. Muscovite has been recognized as a possible replacement candidate. It has similar physical, chemical and electrical properties to Mica; however, it is marketed for use in aqueous systems.

Currently, the ohmic heater's power supply is manually controlled with a variable output transformer. It is highly recommended that the heater's supply be incorporated into a remotely located, fully automated control system. A simple PID controller coupled with a programmable logic controller could be employed which monitors the CHTL system's critical process parameters including temperatures and pressures. Prior consultations with application engineers in the pulsed electric field industry suggest that advanced circuitry could be used to eliminate electrical arching altogether. Nano-second data capture and processing controllers could be used to monitor and override the voltage supply to the heater when unwanted current surges are detected indicating the heater's electrodes may be approaching an unwanted discharge.

Incorporation of more complex electrically regulated circuitry would also allow to the user to test various supply current cycles. In this work only a 60 Hz alternating current power supply was used. Other studies have shown the benefits of employing high frequency inverters in the range of 100-10,000 Hz to reduce the previously observed passivation effects on metal electrodes. Overall improvements of the employed electrodes may be noticed with high frequency power supplies. The efficacy of direct current supplies could also be evaluated.

Improvements to the system's overall process design could also be implemented. Economizing heat exchangers could be employed before the tube-in-tube condenser to capture and recycle process heat. This would greatly reduce the electric load required by the system. Additionally, efforts made to increase the overall capacity and throughput of the system would provide access to additional high pressure processing equipment. Finding suitable equipment for the targeted flowrates of the current CHTL system was difficult. This was especially true for the high pressure process pump in which only HPLC grade pumps were available.

The necessary safety precautions were always followed during these experiments; however, this is increasingly challenging as new components are added to the system and as it is scaled up. Ideally, an isolated processing room should be used for continued research. This would greatly reduce system exposure to the operator, but more importantly, limit the risk to nearby lab members who may be unfamiliar with the conditions inherently involved with HTL processing. Only a few modifications would be needed to fully remotely operate the system, although this would require a significant investment in time and resources. Nonetheless, a few safety improvements remain and they are highly recommended should the decision be made to scale up the system further.

Should work continue with further development the heater, a 3 phase design would greatly enhance its applicability to industrial processes. While the benefits of 3 phase power are numerous, it should be noted that the final prototype design was optimized for single phase 0-280 VAC with one line and one neutral lead only. This should not be confused with other more common forms of single phase sources including 208, 220 and 240 from three phase plugs. Additionally, split single phase sources, common in residential homes, are also not compatible with the final prototype since these single phase sources have two line leads. Ideally, a universal geometry should be devised which alleviates the requirement of explicitly knowing which electrical supplies are compatible with the device in the future iterations.

BIBLIOGRAPHY

112th Congress 1st Session. (2011, September 15). S.1564 Renewable Fuel Parity Act of 2011.

Aitani, A. M. (2004). Oil refining and products. *Encyclopedia of Energy*.

Akhtar, J., & Amin, N. (2011). A review on process conditions for optimum bio-oil yield in hydrothermal liquefaction of biomass. . *Renewable and Sustainable Energy Reviews.*, 1615-1624.

Amin, S. (2009). Review on biofuel oil and gas production processes from microalgae. *Energy Conservation and Management*, 1834-1840.

Antal Jr, M., Leesomboon, T., Mok, W., & Richards, G. N. (1991). Mechanism of formation of 2-furaldehyde from D-xylose. *Carbohydrate Research*, 71-85.

Asghari, F. S., & Yoshida, H. (2006). Acid-catalyzed production of 5-hydroxymethyl furfural from D-fructose in supercritical water. *Industrial & Engineering Chemistry Research.*, 2163-2173.

Berl, E. (1944). Production of oil from Plant Material. *Science*, 309-312.

Biller, P., & Ross, A. B. (2011). Potential yields and properties of oil from hydrothermal liquefaction of microalgae with different biochemical content. . *Bioresource Technology*, 215-225.

Bobleter O. (1994). Hydrothermal degradation of polymers derived from plants. *Polymer Science*, 797-841.

Boocock, D., & Sherman, K. (2009). Further aspects of powdered poplar wood liquefaction by aqueous pyrolysis. . *Can J Chem Eng*, 627-633.

Brandt, A. R., & Farrell, A. E. (2007). Scraping the bottom of the barrel: greenhouse gas emission concequences of a transition to low-quality and synthetic petroleum resources. *Climate Change*, 241-263.

Buhler, W., Dinjus, E., Ederer, H., Kruse, A., & Mas, C. (2002). Ionic reactions and pyrolysis of glycerol as competing reaction pathways in near- and supercritical catalytic dehydration of biomass-derived polyols in sub- and supercritical water. *Journal of Supercritical Fluids.*, 37-53.

Chen, P., Min, M., Chen, Y., Wang, L., Li, Y., Chen, Q., et al. (2009). Review of biological and engineering aspects of algae to fuel approach. *Int J Agric & Biol Eng*, 1-30.

Delmer, D., & Amor, Y. (1995). Cellulose biosythesis. *Plant Cell.*, 987-1000.

Demirbas, A. (2009). Pyrolysis of Biomass for Fuels and Chemicals. *Energy Sources Part A*, 1028-1037.

Demirbas, A. (2010). Hydrogen from Mosses and Algae via Pyrolysis and Steam Gasification. *Energy Sources, Part A* , 172-179.

Demirbas, M. F., Balat, M., & Balat, H. (2011). Biowastes-to-biofuels. *Energy Conversion and Management.*, 1815-1828.

Elliott, D., & Schiefelbein, G. (1989). Liquid hydrocarbon fuels from biomass. *American Chemical Society, Division of Fuel Chemisty Annual Meeting Preprints.*, 1160-1166.

Ferro Ceramic Grinding Inc. (n.d.). *Ceramic Properties Tables*. Retrieved 06 01, 2012, from http://www.ferroceramic.com/macor_table.htm

Ginzburg, B.-Z. (1993). Liquid fuel (oil) from halophilic algae: A renewable source of non-polluting energy. . *Renewable Energy*, 249-252.

Goudriaan, F., Van De Beld, B., Boerefijn, F. R., Bos, G. M., Naber, J. E., Van Der Wal, S., et al. (2000). Thermal efficiency of the HTU® process for biomass liquefaction. *Progress in Thermochemical Biomass Conversion*, 1312-1325.

GTM Research. (2009). Algae Bloom. *The Greentech Innovation Report*, 1-13.

Kabyemela, B., Adschiri, T., Malaluan, R., & Arai, K. (1999). Glucose and fructose decomposition in subcritical and supercritical water: Detailed reaction pathway, mechanisms, and kinetics. *Industrial & Engineering Chemisty Reseach*, 2888-2895.

Karagoz, S., Bhaskar, T., Muta, A., & Sakata, Y. (2005). Comparative studies of oil compositions produced from sawdust, rice husk, lignin and cellulose by hydrothrmal treatment. *Fuel*, 875-884.

Karagoz, S., Bhaskar, T., Muta, A., & Sakata, Y. (2006). Hydrothermal upgrading of biomass: effect of K2CO3 concentration and biomass/water ratio on products distribution. *Bioresource Technology.*, 90-98.

Karagoz, S., Bhaskar, T., Muta, A., Sakata, Y., & Azhar, U. (2004). Low-temperature hydrothermal treatment of biomass: effect of reaction parameters on products and boiling point distributions. . *Energy Fuels*, 234-241.

Karagoz, S., Bhaskar, T., Muta, A., Sakata, Y., Oshiki, T., & Kishimoto, T. (2005). Low-temperature catalytic hydrothermal treatment of wood biomass: analysis of liquid products. *Chemical Engineering Journal*, 127-137.

Kharecha, P. A., & Hansen, J. E. (2008). Implications of "peak oil" for atmospheric CO2 and climate. *Global Biogeochemical Cycles.*

King, J., Holliday, R., & List, G. (1999). Hydrolysis of soybean oil in a subcritical water flow reactor. *Green Chemistry*, 261-264.

Klingler, D., Berg, J., & Vogel, H. (2007). Hydrothermal reactions of alanine and glycine in sub- and supercritical water. *Journal of Supercritical Fluids.*, 112-119.

Li, H., Yuan, X., Zeng, G., Tong, J., & Yan, Y. (2009). Liquefaction of rice straw in sub and supercritical 1,4-dioxane-water mixture. *Fuel Process Technology.*, 657-663.

Luijkx, G., van Rantwijk, F., & van Bekkum, H. (1993). Hydrothermal formation of 1,2,4-benzenetriol from 5-hydroxymethyl-2-furaldehyde and D-Glucose. *Carbohydrate Research.* , 131-139.

McKendry, P. (2002). Energy production from biomass (part 2): conversion technologies. *Bioreseource Technology*, 47-54.

Miao, X., Wu, Q., & Yang, C. (2004). Fast pyrolysis of mcroalgae to produce renewable fuels. . *Journal of Analytical and Applied Physics.*, 855-863.

Mok, W., & Antal, M. (1992). Uncatalyzed solvolysis of whole biomass hemicellulose by hot compressed liquid water. *Industrial Engineering and Chemisry Research.*, 1157-1161.

Nagamori, M., & Funazukuri, T. (2004). Glucose production by hydrolysis of starch under hydrothermal conditions. *Journal of Chemical Technology and Biotechnology.*, 229-233.

Ocfemia, K., Zhang, Y., & Funk, T. (2006). Hydrothermal Processing of Swine Manure Into Oil Using a Continuous Reactor System: Development and Testing. *Transactions of the ASABE*, 533-541.

Ocfemia, K., Zhang, Y., & Funk, T. (2006). Hydrothermal Processing of Swine Manure to Oil Using a Continuous Reactor System: Effects of Operating Parameters on Oil Yield and Quality. *Transactions of the ASABE*, 1897-1904.

Office of Transportation and Air Quality. (2010). *EPA Finalizes Regulations for the National Renwable Fuel Standard Program for 2010 and Beyond.* United States Environmental Protection Agency.

Peterson, A. A., Vogel, F., R., P. L., Froling, M., Antal, M. J., & Tester, J. W. (2008). Thermochemical biofuel production in hydrothermal media: A review of sub- and supercritial water technologies. . *Energy and Environmental Science* , 32-65.

Rogalinski, T., Liu, K., Albrecht, T., & Brunner, G. (2008). Hydrolysis kinetics of biopolymers in subcritical water. *Journal of Supercritical Fluids.*, 335-341.

Ruan, R., Ye, X., Chen, P., Doona, C., & Taub, I. (2001). Ohmic Heating. In P. Richardson, *Thermal Technologies in Food Processing* (pp. 241-265). Woodhead Publishing.

Sasaki, M., Fang, Z., Fukushima, Y., Adschiri, T., & Arai, K. (2000). Dissolution and hydrolysis of cellulose in subcritical and supercritical water. *Industrial & Engineering Chemistry Research*, 2883-2890.

Schnepf, R., & Yacobucci, B. D. (2010). Renewable Fuel Standard (RFS): Overview and Issues. *Congressional Research Service*.

Sharma, Y. C., & Singh, B. (2009). Development of biodiesel: Current scenario. *Renewable and Sustainable Energy Reviews*, 1646-1651.

Sheehan, J., Dunahay, T., Benemann, J., & Paul, R. (1998). *A Look Back at the U.S. Department of Energy's Aquatic Species Program: Biodiesel from Algae.* Golden, CO: National Renewable Energy Laboratory.

Singh, P. R., & Heldman, D. (2008). Introduction to Food Engineering.

Small, K., & Dender, K. V. (2007). Long Run Trends in Transport Demand, Fuel Price Elasticities and Implications of the Oil Outlook for Transport Policy. *Interational Transport Forum*, 2-38.

Toor, S. S., Rosendahl, L., & Rudolf, A. (2011). Hydrothermal liquefaction of biomass: A review of subcritical water technologies. . *Energy.*, 2328-2342.

U.S. DOE. (2010). *National Algal Biofuels Roadmap.* U.S. DOE Biomass Office of Energy Efficiency and Renewable Energy, Biomass Program.

U.S. Energy Information Administration. (2011). *Annual Energy Overview: Petroleum and Other Liquids.* Washington DC: U.S. Department of Energy.

Ueno, Y., Kurano, N., & Miyachi, S. (1998). Ethanol production by dark fermentation in marine green alga, Chlorococcum littorale. *Journal of Fermentation and Bioengineering*, 38-43.

Vardon, D. R., Sharma, B., Scott, J., Yu, G., Wang, Z., Schideman, L., et al. (2011). Chemical properties of biocrude oil from hydrothermal liquefaction of Spirulina algae, swine manure and digested anaerobic sludge. . *Bioresource Technology*.

Wang, G., Li, W., Li, B., & Chen, H. (2007). Direct liquefaction of sawdust under syngas. *Fuel.*, 1587-1593.

Watanabe, M., Iida, T., & Inomata, H. (2006). Decomposition of long chain saturated fatty acid with some additives in hot compressed water. . *Energy Conversion and Management.*, 3344-3350.

Xu, H., Miao, X., & Wu, Q. (2006). High quality biodiesel production from a microalga Chlorella protothecoides by heterotrophic growth in fermenters. *Journal of Biotechnology*, 499-507.

Yin, S., Dolan, R., Harris, M., & Tan, Z. (2010). Subcritical hydrothermal liquefaction of cattle manure to bio-oil: Effects of conversion parameters on bio-oil yield and characterization of bio-oil. *Bioresource Technology*, 3657-3664.

Zhang, B., Keitz, M., & Valentas, K. (2009). Thermochemical liquefaction of high-diversity grassland perennials. . *Journal of Applied and Analytical Pyrolysis.*, 18-24.